Precambrian Research 164 (2008) 137–159

Contents lists available at ScienceDirect

Precambrian Research

journal homepage: www.elsevier.com/locate/precamres

Paleomagnetism and Detrital Zircon Geochronology of the Upper Vindhyan Sequence, Son Valley and Rajasthan, India: A ca. 1000 Ma Closure age for the Purana Basins?

S.J. Malone[a], J.G. Meert[a,*], D.M. Banerjee[b], M.K. Pandit[c], E. Tamrat[a], G.D. Kamenov[a], V.R. Pradhan[a], L.E. Sohl[d]

[a] Department of Geological Sciences, University of Florida, 241 Williamson Hall, Gainesville, FL 32611 USA
[b] Department of Geology, University of Delhi, Delhi 110007, India
[c] Department of Geology, University of Rajasthan, Jaipur 302004, Rajasthan, India
[d] CCSR/GISS at Columbia University, 2880 Broadway, New York, NY 10025, USA

ARTICLE INFO

Article history:
Received 20 December 2007
Received in revised form 21 March 2008
Accepted 21 April 2008

Keywords:
Vindhyan
Bhander, Rewa
East Gondwana
Rodinia
India

ABSTRACT

The utility of paleomagnetic data gleaned from the Bhander and Rewa Groups of the "Purana-aged" Vindhyanchal Basin has been hampered by the poor age control associated with these units. Ages assigned to the Upper Vindhyan sequence range from Cambrian to the Mesoproterozoic and are derived from a variety of sources, including $^{87}Sr/^{86}Sr$ and $\delta^{13}C$ correlations with the global curves and Ediacara-like fossil finds in the Lakheri–Bhander limestone. New analyses of the available paleomagnetic data collected from this study and previous work on the 1073 Ma Majhgawan kimberlite, as well as detrital zircon geochronology of the Upper Bhander sandstone and sandstones from the Marwar SuperGroup suggest that the Upper Vindhyan sequence may be up to 500 Ma older than is commonly thought. Paleomagnetic analysis generated from the Bhander and Rewa Groups yields a paleomagnetic pole at 44°N, 214.0°E (A95 = 4.3°). This paleomagnetic pole closely resembles the VGP from the well-dated Majhgawan intrusion (36.8°N, 212.5°E, α_{95} = 15.3°).

Detrital zircon analysis of the Upper Bhander sandstone identifies a youngest age population at ~1020 Ma. A comparison between the previously correlated Upper Bhander sandstone and the Marwar sandstone detrital suites shows virtually no similarities in the youngest detrital suite sampled. The main 840–920 Ma peak is absent in the Upper Bhander. This supports our assertion that the Upper Bhander is older than the 750–771 Ma Malani sequence, and is likely close to the age of the 1073 Ma Majhgawan kimberlite on the basis of the paleomagnetic similarities. By setting the age of the Upper Vindhyan at 1000–1070 Ma, several intriguing possibilities arise. The Bhander–Rewa paleomagnetic pole allows for a reconstruction of India at 1000–1070 Ma that overlaps with the 1073 ± 13.7 Majhgawan kimberlite VGP. Comparisons between the composite Upper Vindhyan pole (43.9°N, 210.2°E, α_{95} = 12.2°) and the Australian 1071 ± 8 Ma Bangamall Basin sills and the ~1070 Ma Alcurra dykes suggest that Australia and India were not adjacent at this time period.

1. Introduction

The cratonic blocks of East Gondwana represent an important element of Proterozoic paleogeographic reconstructions and tectonic studies. Included in these cratonic blocks are the Rayner and Mawson cratonic blocks (East Antarctica), Australia, Madagascar, the Seychelles, Sri Lanka and India (Meert, 2003; Powell and Pisarevsky, 2002). Fig. 1, modified from Gray et al. (in press), shows the position of these cratons, as well as orogenic belts associated with their assembly, in the Gondwana supercontinent configuration. In particular, there has been a good deal of debate concerning their configuration in the Mesoproterozoic supercontinent of Rodinia, as well as their subsequent coalescence in the continent of Gondwana following the Neoproterozoic breakup of Rodinia (e.g. Meert and Van der Voo, 1996; Rogers et al., 1995; Weil et al., 1998; Powell and Pisarevsky, 2002; Meert, 2003; Meert and Torsvik, 2003; Veevers, 2004; Collins and Pisarevsky, 2005; Squire et al., 2006; Meert and Lieberman, 2008)

The paucity of high quality paleomagnetic data hinders the reconstructions and the refinement of APW paths of these units

* Corresponding author. Fax: +1 352 392 9294.
E-mail addresses: sjmalone@ufl.edu (S.J. Malone), jmeert@ufl.edu (J.G. Meert).

0301-9268/$ – see front matter © 2008 Elsevier B.V. All rights reserved.
doi:10.1016/j.precamres.2008.04.004

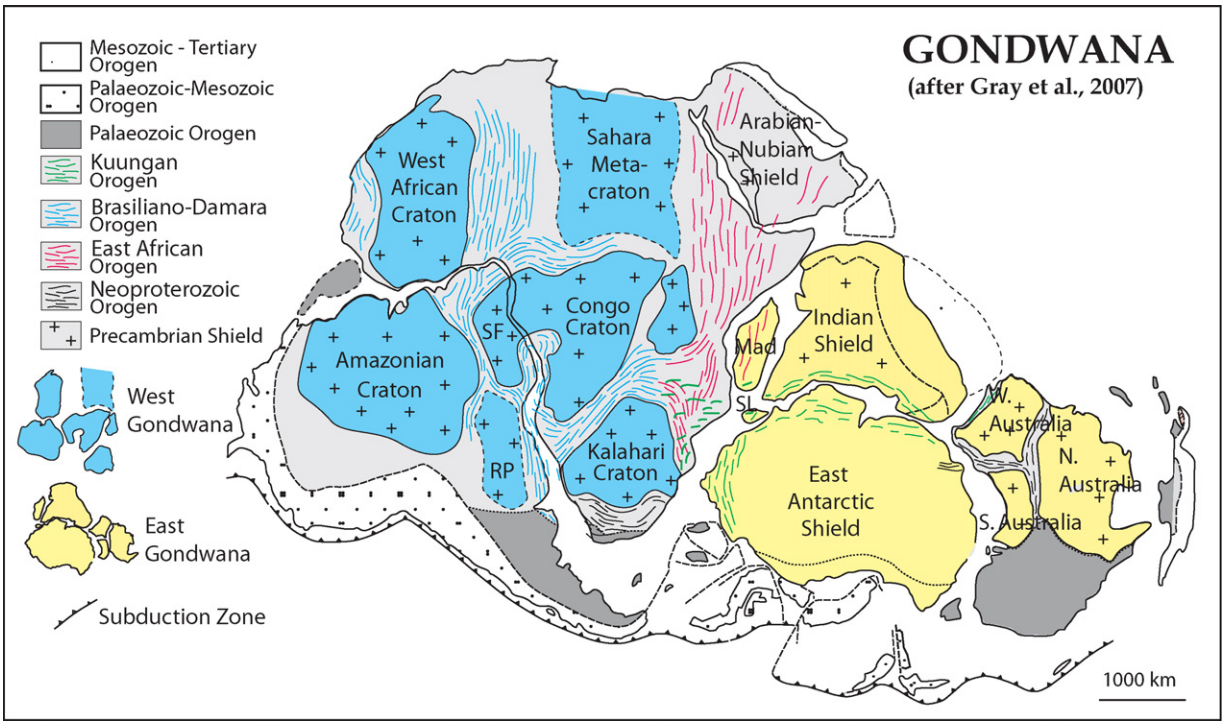

Fig. 1. "Traditional" Gondwana reconstruction showing Neoproterozoic and younger orogenic belts separating the various elements of East and West Gondwana (modified from Gray et al., in press).

for this critical time interval (Meert and Powell, 2001). Research on the Indian subcontinent provides an important window into this problem as it is both accessible and contains targets of the appropriate age. High quality paleomagnetic and geochronologic data are almost non-existent for India during Meso- to Neoproterozoic times. The Vindhyan Basin (Fig. 2a), located in the central peninsular region of India, provides a promising area to conduct the necessary paleomagnetic studies due to the long depositional history recorded in the basin, limited deformation and unmetamorphosed nature of the rock basin wide. Studies in the Vindhyan Basin, however, are hindered by the poor geochronologic control of the Upper Vindhyan units. These units are separated from the well-dated Mesoproterozoic age Lower Vindhyan by multiple unconformities of indeterminate interval. Any project seeking to use paleomagnetic data generated from the Upper Vindhyan must address the problem of poorly constrained age in the basin. The data ultimately generated by this paper will aid in constraining the position of India during the poorly resolved Meso- to Neoproterozoic interval, generate points that can be used in a Proterozoic APW path for India, and test hypotheses bearing on Rodinia breakup and assembly of East Gondwana.

1.1. Geologic setting

The Vindhyan Basin is a large sedimentary basin located in central peninsular India that outcrops over an area of over 104,000 km^2, with additional area covered by the Deccan Traps and Indo-Gangetic alluvium (Fig. 2a–c; Venkatachala et al., 1996). Geographically, the basin lies between the gneiss and granite of the Archean (>2.5 Ga) Aravalli–Bundelkhand province to the north and east (Mazumdar et al., 2000), and the Cretaceous age Deccan Traps flood basalts to the south. The outcrop area of the Vindhyan Basin is divided into two terrains: the Rajasthan terrain in the present day west region (Fig. 2b), and the Uttar Pradesh–Madhya Pradesh–Bihar region (Fig. 2c) in the eastern sector of the modern day regional extent (Mitra, 1996). Acting as a basement ridge between the Rajasthan and Son Valley terrains (Prasad and Rao, 2006) are the trondhjemitic gneisses of the 2600–2500 Ma Bundelkhand Igneous complex (Sarkar et al., 1995). The Bundelkhand granite, considered to be the terminal event in the Bundelkhand complex, is dated at 2492 ± 10 Ma by Mondal et al. (2002). The Great Boundary Fault of the Rajasthan section separates the weakly deformed and unmetamorphosed Vindhyan system sediments from older, deformed Aravalli SuperGroup and provides a western boundary for the Rajasthan section of the basin. Across the modern day Aravalli Mountains is the 54,000 km^2 750–771 Ma Malani Igneous Province, and unconformably overlying sediments of the Neoproterozoic–Cambrian Marwar SuperGroup (Raghav et al., 2005). The Marwar SuperGroup is represented by undeformed to mildly folded sediments up to 2 km in thickness (Roy, 2001). The lower age for the Marwar SuperGroup is constrained to be younger than the Malani Igneous Province and is generally assumed to continue into the latest Neoproterozoic (Chaudhuri et al., 1999; Raghav et al., 2005). A few modern day drainages cross through this region onto the Vindhyan outcrop area. To the east, the Vindhyan Basin is separated from Paleoproterozoic rock by the Narmada–Son Lineament (Prasad and Rao, 2006).

The Vindhyan Basin is one of a Group of Proterozoic basins in the Indian subcontinent referred to as Purana ("Ancient") Basins. These Purana Basins are thought to represent the infill of failed rifts that developed on earlier Archean and/or early Paleoproterozoic cratonic blocks (Ram et al., 1996; Chaudhuri et al., 2002). The Vindhyan Basin formed on the Aravalli craton, which stabilized by 2.5 Ga (Mondal et al., 2002). Rifting thinned part of the crust along a series of east to west trending faults in a dextral transtensional setting (Bose et al., 2001). Rift related features are common in the lower parts of the section, including volcaniclastic units, faults, and paleoseismic sedimentary deformation (Bose et al., 2001). The rift origin of these basins is supported by a variety of data but still the source of some controversy. The basins are bounded by faults visible

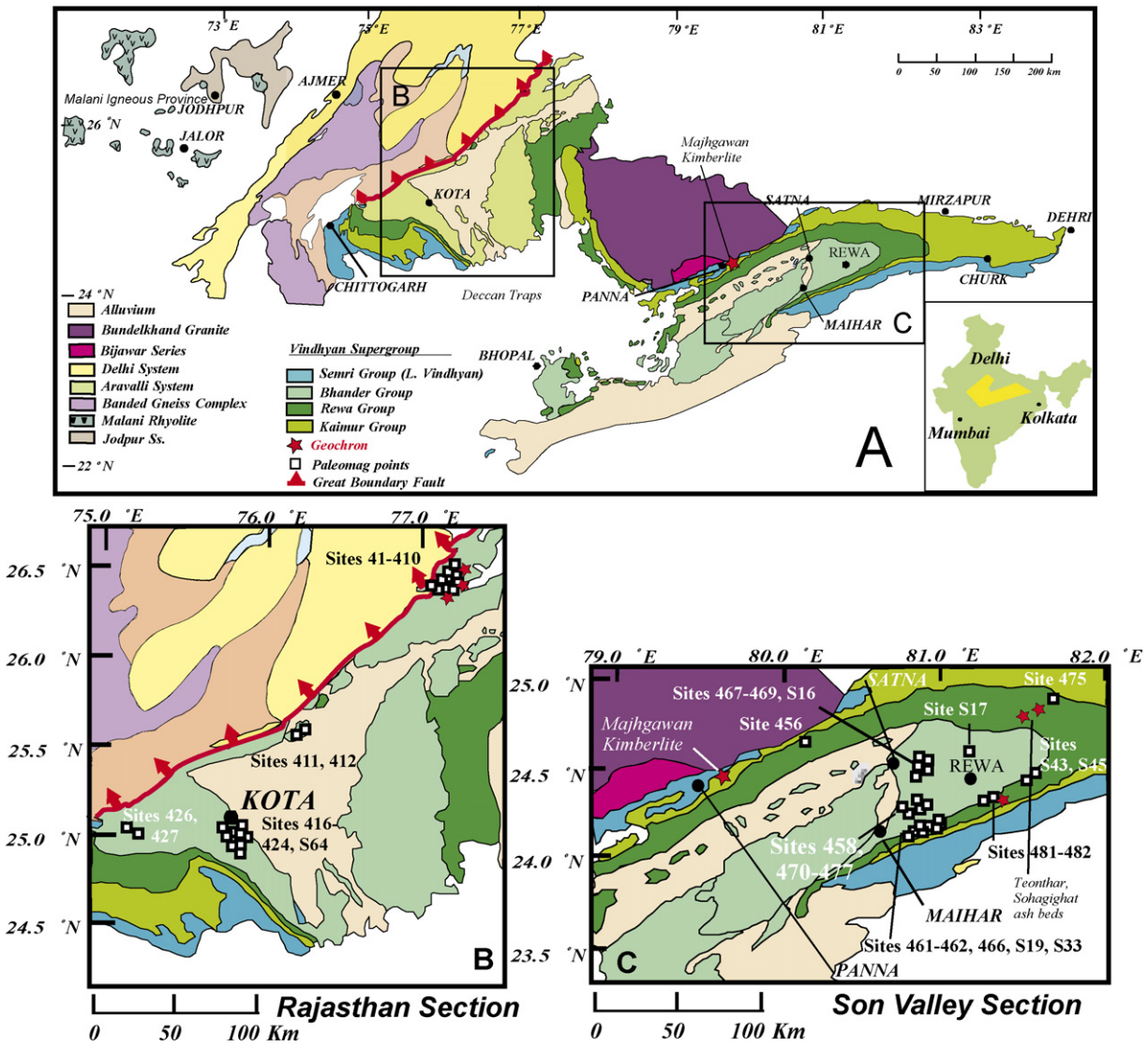

Fig. 2. Generalized geological map of the Vindhyanchal Basin showing (a) regional overview (b) close-up of the Rajasthan section and (c) close-up of the Son Valley section of the basin.

on seismic profiles, gravity data, and geologic mapping (Prasad and Rao, 2006; Ram et al., 1996; Chaudhuri et al., 2002). Periodic volcanic events deposited volcaniclastic layers preserved in the basins (Chakraborty et al., 1996; Chaudhuri et al., 2002). Basin wide unconformities, sedimentation disturbances, and changes in paleoslope level indicate tectonic changes in the fault block underlying the basin (Prasad and Rao, 2006; Chaudhuri et al., 2002). For the most part, the sediments of the Vindhyan Basin are undeformed to mildly deformed, and typically show low dips except in areas of Cenozoic faulting.

1.2. Stratigraphy

Sedimentary units in the Vindhyan Basin are primarily represented by shallow marine facies along with distal shelf to deep-water sediments in the Lower Vindhyan and Lower Rewa, and can be subdivided into four Groups: The Semri (or "Lower Vindhyan" sequence), Kaimur, Rewa and Bhander (forming the "Upper Vindhyan" sequence) (Chaudhuri et al., 1999). The Lower Vindhyan and Upper Vindhyan units are separated by multiple unconformities of undetermined duration (Bose et al., 2001). There is also evidence of an unconformity at, or near, the top of the Kaimur Group. Fig. 3 outlines this general stratigraphy.

The lower Vindhyan units are collectively designated the Semri Group. The Semri sediments unconformably overlie basement rock of either the 1854 ± 7 Ma Hindoli Group (Deb et al., 2001) or the 2492 ± 10 Ma Bundelkhand granites (Mondal et al., 2002). The Semri Group in the Son Valley overlies the Bijawar series of sediments and lavas, which contains volcanic rocks that Mathur (1981) correlates to the 1815 Ma Gwalior volcanics. Prasad and Rao (2006) suggest that the Gwalior and Bijawar series form an extensive part of the basement, as well as offering geophysical data that suggest the Hindoli Group extends beneath the Rajasthan section of the Vindhyanchal Basin. The Semri Group consists of five formations and is typically alternating shale and carbonate units, with areas of sandstone and volcaniclastic units. The Semri is noteworthy for good age control from Pb–Pb ages from carbonate units, as well as precise U–Pb ages derived from zircon separated from volcaniclastic strata (Ray et al., 2002; Rasmussen et al., 2002a).

The Semri Group is separated from the Upper Vindhyan by a basin wide unconformity between the Rohtas limestone and the overlaying Kaimur Group. The Kaimur consists of a lower shale unit

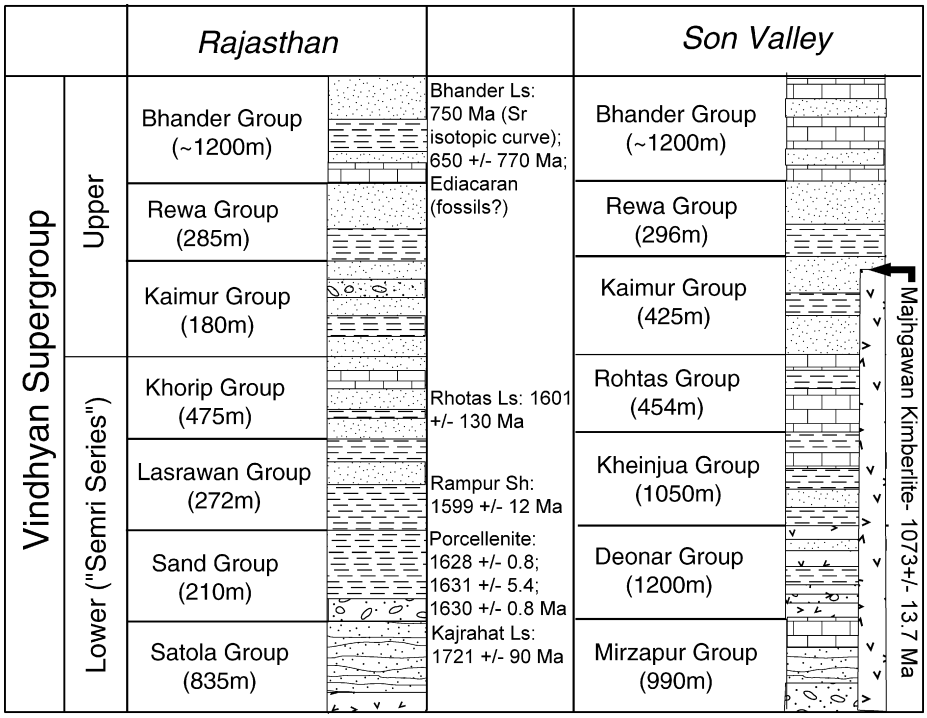

Fig. 3. Generalized stratigraphy and correlations of the Vindhyan SuperGroup for the Son Valley and Rajasthan sections. Age determinations from Gregory et al. (2006), Sarangi et al. (2004), Ray et al. (2003, 2002) and De (2006).

overlain by quartz rich sandstone including a volcaniclastic deposit (Bose et al., 2001). This unit is intruded by the 1073 ± 13.7 Ma Majhgawan kimberlite (Gregory et al., 2006), which cross-cuts the Semri and Kaimur Groups and is currently exposed in the Kaimur Group (Baghain) sandstone in the vicinity of Panna, Madhya Pradesh (Fig. 2c). Up-section is the Rewa Group, a series of shale and sandstone formations that, in areas, contain kimberlite derived diamondiferous conglomerates (Rau Soni, 2003). There is uncertainty with regard to the source of these conglomerates, as Rau Soni (2003) suggests that the diamonds present in the conglomerate may not be derived from the proximal Majhgawan or Hinota kimberlites. The conglomerate is succeeded by a shale unit, which in turn is succeeded by the Rewa sandstone. A thin shale unit marks the transition into the Bhander Group. The Bhander Group contains the only major carbonate unit in the upper Vindhyan system, a unit containing stromatolites, ooids, and micritic layers known as the Bhander or Lakheri limestone (Bose et al., 2001). The overlying lower Bhander sandstone marks a transition into shallower marine, sometimes fluvial, sandstone typical of the Bhander Group (Bose et al., 2001). The Sirbu shale overlies the lower Bhander sandstone, and is in turn overlain by the upper Bhander sandstone. Bose et al. (2001) observed that the upper Bhander sandstone is primarily a unit of coarse, red sandstones, and may represent former barrier islands, sand bars, beaches and fluvial systems (Akhtar, 1996).

2. Previous work

2.1. Temporal controls on the vindhyanchal basin sedimentation

The age of deposition in the Vindhyanchal Basin has been debated for over 100 years (e.g. Oldham, 1893; Auden, 1933; Crawford and Compston, 1970; Venkatachala et al., 1996). Due to the general absence of fossils suitable for biostratigraphic dating, ages for the various Vindhyan units has been assigned by radiometric means where possible. Early radiometric age dates depended on K–Ar, Rb–Sr, and fission track methods on detrital or authigenic minerals or on kimberlite intrusions that cross cut the Vindhyanchal Basin; later work focused on dating volcaniclastic deposits, putative fossil evidence, or global isotopic correlations (e.g. Vinogradov et al., 1964; Tugarinov et al., 1965; Crawford and Compston, 1970; Paul et al., 1975; Paul, 1979; Srivastava and Rajagopalan, 1988; Smith, 1992; Kumar et al., 1993; Miller and Hargraves, 1994; Venkatachala et al., 1996; Rasmussen et al., 2002a,b; Ray et al., 2002, 2003; Sarangi et al., 2004; De, 2003, 2006). For the most part, these studies limited the age of the Lower Vindhyan Semri Group to older than 1.1 Ga. Younger glauconite and fission track dates used in many studies may reflect post-depositional thermal or chemical resetting (Rasmussen et al., 2002a,b; Deb et al., 2001).

Basement age control, as noted above, is primarily based on U–Pb analysis of zircon separated from the 2530 ± 3.6 Ma Berach granite (Tucker, personal communication), 2492 ± 10 Ma Bundelkhand granite (Mondal et al., 2002), the maximum age of 2240 Ma for the Khairmalia felsite (Tucker, personal communication), and the1854 ± 7 Ma Hindoli Group (Deb et al., 2002). Lower Vindhyan Semri Group ages are generally well constrained. The Kajrahat limestone yielded a Pb–Pb age of 1721 ± 90 Ma (Sarangi et al., 2004). Rasmussen et al. (2002a) and Ray et al. (2002) have published consistent U–Pb ages taken from magmatic zircons. Zircon grains separated from ash beds located in the Rampur shale give ages of 1602 ± 10 and 1593 ± 12 Ma, and those from the Deonar/Porcellanite formation yield an age of 1628 ± 8 Ma (Rasmussen et al., 2002a). Further constraints published by Ray et al. (2002) from the Deonar/Porcellanite formation showed U–Pb zircon ages of 1630 ± 5.4 and 1631 ± 0.8 Ma. Pb–Pb dating on the Rohtas limestone has yielded two ages, 1599 ± 48 (Sarangi et al., 2004) and 1601 ± 130 Ma (Ray et al., 2003). These age constraints are summarized in Table 1.

Age control on the Upper Vindhyan sequences is more problematic. The best age estimates come from the Majhgawan kimberlite,

Table 1
Recent age constraints for the Vindhyanchal Basin

Unit	Age	Method	Reference
Upper Vindhyan			
Bhander Group ages			
Lakheri Ls., Rajasthan	Ediacaran	Fossils (?)	De (2003, 2006)
Lakheri Ls., Rajasthan	650 Ma	Sr isotope stratigraphy	Ray et al. (2003)
Bhander Ls., Son Valley	650 ± 770 Ma	Pb–Pb Isochron	Ray et al. (2002)
	750 Ma	Sr isotope stratigraphy	Ray et al. (2003)
	700–1100 Ma	Chuaria-Tawunia fossils	Kumar and Srivastava (1997)
Rewa Group ages			
Jhiri Shale (Rewa group) Son Valley	700–1100 Ma	Chuaria-Tawunia fossils	Rai et al. (1997)
Kaimur Group ages (Majhgawan kimberlite intrusion)			
Majhgawan kimberlite, which intrudes the Kaimur group (Baghain Ss.) near Panna	1044 ± 22 Ma	Rb–Sr (Phlogopite)	Smith (1992)
	1067 ± 31 Ma	Rb–Sr (Phlogopite)	Kumar et al. (1993)
	1073.5 ± 13.7 Ma	Ar–Ar (Pholgopite)	Gregory et al. (2006)
Lower Vindhyan			
Semri Group ages			
Rhotas Ls. (Semri Group)	1599 ± 48 Ma	Pb–Pb Isochron	Sarangi et al. (2004)
(Son Valley)	1601 ± 130 Ma	Pb–Pb Isochron	Ray et al. (2003)
Glauconite Ss. (Chorhat Ss, Semri grp)	1504–1409 Ma	Rb–Sr (Glaconite)	Kumar (2001)
Rampur Shale (Semri Group)	1599 ± 8 Ma	U–Pb (Zircon)	Rasmussen et al. (2002a,b)
Porcellanite Fm (Semri Group)	1628 ± 8 Ma	U–Pb (Zircon)	Rasmussen et al. (2002a,b)
(Son Valley)	1630.7 ± 0.4 Ma	U–Pb (Zircon)	Ray et al. (2002)
Kajrahat Ls (Semri Group)	1721 ± 90 Ma	Pb–Pb Isochron	Sarangi et al. (2004)
Basement			
Hindoli Group volcanics	1854 ± 14 Ma	U–Pb (Zircon)	Deb et al. (2002)
Khairmalia felsite	2240 Ma (Max)	U–Pb (Zircon)	Tucker (personal communication)
Bundlekhand Granite	2492 ± 10 Ma	Pb–Pb (Zircon)	Mondal et al. (2002)
Berech Granite	2530 ± 3.6 Ma	U–Pb (Zircon)	Tucker (personal communication)

that intrudes the Lower Vindhyan and into the Baghain sandstone (Kaimur Group) near Panna. The kimberlite was first dated using K–Ar and Rb–Sr methods, yielding dates between 1170 and 947 Ma (Paul et al., 1975). Rb–Sr ages include Crawford and Compston (1970), at 1140 ± 12 Ma, Smith (1992) with an age of 1044 ± 22 Ma, and Kumar et al. (1993) with an age of 1067 ± 31 Ma. Most recently, the Majhgawan kimberlite has been dated by Gregory et al. (2006) at 1073.5 ± 13.7 Ma via ^{40}Ar–^{39}Ar analysis of phlogopite phenocrysts, and is the reference date used in this study. Ages from within the Upper Vindhyan sedimentary units lack consistency and reliability. The Kaimur sandstone has a reported K–Ar age on authigenic glauconite of 910 ± 39 Ma (Vinogradov et al., 1964) that is too young in light of the age of the Majhgawan kimberlite that intrudes it. Fission track ages from the Govindgarh sandstone (upper Rewa Group) yield a date of 710 ± 120 Ma (Srivastava and Rajagopalan, 1988). Recent Pb–Pb dating of Bhander Group carbonates produce an unreliable date of 650 ± 770 Ma; however, this age appears consistent with samples taken from the Bhander–Lakheri limestone that yields a $^{87}Sr/^{86}Sr$ value consistent with global values near 650 Ma (Ray et al., 2003). Further isotopic studies of the Bhander limestone $^{87}Sr/^{86}Sr$ values indicate a 750 Ma age when compared to global curves for the Neoproterozoic (Ray et al., 2003). $\delta^{13}C$ values for the limestone units show some overlap with the ages inferred by $^{87}Sr/^{86}Sr$ isotopic curves and also show some negative values which Ray et al. (2003) suggest may be evidence of Neoproterozoic glaciations.

Non-isotopic methods of dating the Upper Vindhyan units have also been attempted, with equivocal results. Possible Ediacara fauna fossils of nine coelenterate genera (*Tribachidium*, *Eoporita*, *Kaisalia*, *Cyclomedusa*, *Ediacaria*, *Nimbia*, *Paliella*, *Medusinites*, *Hiemaloria*), one proto arthropod (*Spriggina*) and several unidentified taxa have been described in the Lakheri and Sirbu formations of the Bhander Group and would indicate an Ediacaran age (<635 Ma) for the Bhander (De, 2003, 2006). This fauna is useful both for the biostratigrapic age constraint as well as for correlations with other Ediacara sites worldwide (De, 2006). Other occurrences from India, Canada and Namibia show similar facies control on the distribution of Ediacara fossils, with preservation maximized in siliciclastic units and absent in intervening stromatolitic carbonate beds (De, 2006). Waggoner (1999, 2003) notes that Ediacara fauna typically fall into one of three broad, regionally defined Groups: Group one, diagnostic of Baltica, Siberia, northern Laurentia, and Australia; Group two, diagnostic of Namibia, the South American Ediacara occurrences, and southern Laurentia; and Group three, restricted to the Avalonia terrane preserved in the present Carolina Slate Belt, Newfoundland and the Charnwood Forest site of Great Britain. Meert and Lieberman (2008) observe that the fauna described by De (2003, 2006) appears to fit best in the Group 1 category (White Sea fauna).

Fossil evidence in the Vindhyan Basin has proven problematic in the past, as exhibited by the controversial triploblastic animal traces from the Semri Group described by Seilacher et al. (1998), which were claimed to push back the age of metazoan development. Azmi (1998) added to the controversy with his reports of brachiopods and small shelly fauna (SSF) in the Chorhat sandstone (Semri Group). Further research into the age of the Lower Vindhyan sediments yielded robust Paleoproterozoic-Mesooproterozoic ages (Ray et al., 2002; Rasmussen et al., 2002a) and makes a Neoproterozoic–Cambrian age for the Chorhat sandstone untenable. However, recent work hints at the possibility that Ediacaran-like fossils may be present in the lower Vindhyan basin extending complex life (though not specifically Ediacarans) into the Paleoproterozoic (Bengtson et al., 2007). These incidents underscore the need for independent verification of Vindhyan fossil finds if major conclusions are to be drawn from them.

Attempts to assign age control to the Upper Vindhyan have also used correlations between paleomagnetic directions from the Group and directions with better age control. Directions obtained from the Bhander and Rewa appear to correlate with late Neoproterozoic to Cambrian data from Pakistan (McElhinny et al., 1978). These correlations are suspect due to significant rotations

in the Salt Range (Klootwijk et al., 1986). Similarities between the Bhander–Rewa paleomagnetic pole and those of other Gondwana cratons have been drawn as well. Many publications (e.g. Meert, 2001; Powell and Pisarevsky, 2002) place the Bhander and Rewa poles on the late Neoproterozoic to Cambrian APW path for Gondwana, assuming a ~550 Ma age for the Upper Vindhyan and comparing the poles to the 547 Ma Sinyai dolerite pole on the Congo craton (Meert and Van der Voo, 1996) or the 645–635 Ma (Kendall et al., 2006; Condon et al., 2005) Elatina–Yaltipena formation poles of Australia from Schmidt and Williams (1995) and Sohl et al. (1999).

2.2. Paleomagnetism

The Vindhyan Basin has been the subject of several paleomagnetic studies. Athavale et al. (1972) treated Upper Bhander and Rewa sandstone samples to alternating fields of up to 80 mT and thermal demagnetization steps up to 600 °C that yielded a Bhander mean direction of $D = 48°$, $I = -19°$, $\kappa = 200$, $\alpha_{95} = 5.7°$ and a Rewa mean of $D = 32°$, $I = -37°$, $\kappa = 15$, $\alpha_{95} = 13.7°$. These results yielded a paleomagnetic pole of 35°N and 222°E for the Rewa, and 31.5°N and 199°E for the Bhander. Klootwijk (1973) analyzed 43 cores from seven sites in Rajasthan by applying progressive alternating field (AF) and thermal treatments on the samples, and generated a combined site mean of $D = 207.5°$, $I = +9.5°$, $\kappa = 137.5$, $\alpha_{95} = 5.5°$ and a paleomagnetic pole at 51.4°N and 214°E. A later study conducted by McElhinny et al. (1978) expanded sampling into the lower sandstone of the Bhander and included one site in the Rewa Group. In all, seven sites were sampled and subjected to a thermal demagnetization treatment (McElhinny et al., 1978). Three vectors were identified: a viscous component aligned with the present day field, a Tertiary overprint associated with the Deccan Traps emplacement, and a primary direction evident above 600–665 °C (McElhinny et al., 1978). This primary direction, averaged for the seven Bhander–Rewa sites, is: $D = 203.4°$, $I = +8.1°$ ($\kappa = 36.5$, $\alpha_{95} = 11.2°$) with a Rewa VGP at 45.0°N, 191.3°E and a Bhander paleomagnetic pole at 51.3°N, 222.7°E (McElhinny et al., 1978). Paleomagnetism of the Kaimur sandstones, stratigraphically below the Bhander and Rewa sequences, was conducted by Sahasrabudhe and Mishra (1966) and yielded the following direction $D = 357°$, $I = +31°$ ($\alpha_{95} = 6.0°$). Although these samples show several reverse directions, the overall mean is suspiciously close to the local present day field direction ($D = 0$, $I = +42$; Meert and Torsvik, 2003). Poornachandra Rao et al. (2005) obtained somewhat similar directions from the Dhandraul sandstone of the Kaimur Group ($D = 5°$, $I = +42°$, $\kappa = 14.04$, $\alpha_{95} = 13.2°$) and steeper inclinations from Dicken sandstone (Kaimur Group) of $D = 356°$, $I = +62°$ ($\kappa = 35.10$, $\alpha_{95} = 11.8°$). The authors attempt to use these directions to correlate the Kaimur directions (and hence age of the Kaimur) to the Malani Igneous province ($D = 359.1°$, $I = +62°$). This age correlation is negated by the relationship between the Kaimur Group and the 1073 ± 13.7 Ma Majhgawan intrusion, which suggests that the Kaimur magnetization may either represent a Malani like remagnetization or more likely the present day geomagnetic field.

3. Analytical methods

3.1. Paleomagnetism

A total of 56 sites located in Rajasthan and the Son Valley of India were sampled for paleomagnetic study using a water-cooled portable drill. Sample collection covered the sandstones and carbonates of the Bhander and Rewa Groups. Sample orientation was performed in the field using Brunton magnetic compasses, and solar readings were used to correct any magnetic deflections and local declination deviations. The samples were cut into cylindrical specimens of relatively uniform volume in the laboratory. Sample susceptibility was measured on the Sapphire Instruments SI-3B Bridge, and Curie temperature runs were performed incrementally on rock powders in a KLY-3S susceptibility bridge attached to a CS-3 heating unit. Isothermal remnant magnetizations (IRM) were conducted on an ASC Scientific Model IM-10–30 impulse magnetizer. Pilot samples were selected for preliminary demagnetization and a sequence of demagnetization steps was chosen based on these preliminary results. Sandstone samples were treated with stepwise thermal demagnetization. Magnetite bearing limestone samples were treated with initial low temperature treatments in the form of liquid N_2 baths (Dunlop and Argyle, 1991), followed by alternating fields up to 10–30 mT and stepwise thermal demagnetization or by conventional alternating field (AF) treatments. Thermal demagnetization was carried out using an ASC TD-48 thermal demagnetizer and AF demagnetization treatments used a DTech 2000 AF demagnetizer. All samples were measured on a 2G 77R Cryogenic Magnetometer at the University of Florida. The resulting data was analyzed using principle component analysis of a best fit line on Super IAPD software (Torsvik et al., 2000).

3.2. Geochronology methods

Geochronologic samples from the Rewa Group (Son Valley) Sohagighat and Teonthar ash beds, as well as a possible volcaniclastic bed from the Rajasthan section, were taken in an attempt to provide a more tightly constrained age for the Upper Vindhyan. In addition, detrital zircon grains were separated from Upper Bhander sandstone from paleomagnetic sites 43, 44 and 45 (Fig. 2b) in Rajasthan as well as two sites (Sonia and Girbakhar sandstones) from the Marwar SuperGroup. The ash fall volcaniclastic deposits and sandstones were crushed, disk milled and sieved. The ash fall deposit samples were sieved at 125 μm and rinsed before further processing in heavy liquids, followed by magnetic separation on a Franz Isodynamic separator. Detrital zircons were separated from sandstones via water table treatment, followed by heavy liquids and magnetic separation. Zircon grains were picked from the appropriate fractions (lowest non-magnetic for ash fall grains, non-magnetic at 6°, 1.0 A for detrital grains), were mounted in epoxy plugs, ground, and polished to expose the grains. The plugs were sonicated and cleaned in nitric acid to remove any common Pb surface contamination. Following cleaning, the grains were photographed under a reflected light microscope.

Zircon U–Pb analyses were performed at the Department of Geological Sciences, University of Florida, using "Nu-Plasma" (Nu Instruments, UK) laser ablation multi-collector inductively coupled plasma mass spectrometer (LA-MC-ICP-MS). Mounted zircon grains were laser ablated using an attached New Wave 213 nm ultraviolet laser. A mix of Ar and He carrier gas (1 L/min Ar, 0.5 L/min He) was used for sample transport into the mass spectrometer. The laser was set at 4 Hz pulse frequency, 40% power and a laser spot diameter of 40 μm. Prior to ablation, on-peak background "zero" measurement was taken for 20 s on the blank He and Ar gases with closed laser shutter. This zero is used for on-line correction for isobaric interferences, particularly from ^{204}Hg which is largely derived from the argon gas. Following blank acquisitions, sample ablation proceeded for 30 s in order to minimize ablation pit depth and hence elemental fractionation. Sample analyses were "bracketed" by 2 analyses of FC-1 standard zircon for every 10 unknown zircons. The U–Pb isotopic data were acquired using Nu Instruments Time Resolved Analysis (TRA) software. The TRA software allows for isotopic ratios to be calculated from the desired time segment of data, allowing variations due to grain defects or surface contamination

Table 2
Summary of paleomagnetic data from the Bhander and Rewa groups, Upper Vindhyan sequence

Site	Site Latitude	Site Longitude	*N*	GDec	GInc	SDec	SInc	κ	α_{95}	Pole Lat	Pole Long
U. Bhander Ss.											
Site 41	26°32.877′N	77°02.093′E	6	193.8	21.5	206.8	33.9	117.7	6.2	−37.9°N	44.2°E
Site 42	26°27.816′N	77°02.649′E	4	46.4	−11.4	47.4	−10.8	78.24	10.4	34.7°N	195.8°E
Site 43	26°27.024′N	77°03.334′E	5	237	6.3	227	6.3	73.83	9	−35.8°N	12.8°E
Site 44	26°31.306′N	77°01.052′E	–	–	–	–	–	–	–	–	–
Site 45	26°26.307′N	76°57.163′E	18	204.5	8.9	204.5	10.3	107.3	3.4	−50.5°N	36.5°E
Site 46	26°26.289′N	76°57.482′E	12	201.5	9.7	201.6	11.6	61.31	5.6	−51.5°N	40.9°E
Site 47	26°25.916′N	76°57.269′E	5	204.2	2.7	204	2	36.38	12.9	−54.1°N	33.0°E
Site 48	26°25.902′N	76°57.234′E	12	203.9	11.2	203.8	12.6	32.1	7.8	−48.5°N	38.5°E
Site 49	26°25.840′N	76°57.213′E	6	199.2	4.3	199.2	4.3	111	6.4	−55.9°N	41.0°E
Site 410	26°25.966′N	76°57.184′E	8	198.9	9	198.9	9	104.1	5.5	−54.0°N	43.6°E
Site 64	25° 08.8′N	75°48.1′E	27	33	−37.8	32	−31.7	28	5.4	37.5°N	216.2°E
Sirbu Sh.											
Site 20	24°18.6′N	80° 46.1′E	8	50.5	−41	51	−38	54.1	7.6	21.9°N	211.5°E
Mean Upper Bhander & Sirbu Shale			11			Tilt Corrected		37	7.6	−44.4°N	33.2°E
L. Bhander Ss.											
Site 416	24°48.964′N	75°59.283′E	2	21.1	−5.7	20.2	−11.1	–	–	53.8°N	220.4°E
Site 417	24°48.949′N	75°59.452′E	6	31.4	−10.6	31.2	−26.1	18.16	16.2	40.9°N	214.3°E
Site 418	24°49.237′N	75°00.214′E	9	30.3	−16.1	30.2	−18.6	26.83	10.1	44.7°N	210.7°E
Site 419	25°05.708′N	75°55.071′E	–	–	–	–	–	–	–	–	–
Site 420	25°03.597′N	75°43.382′E	11	19.2	−7.6	19.2	−7.6	12.31	13.6	56.8°N	219.3°E
Site 421	25°04.263′N	75°34.546′E	7	31	−30.1	31	−30.1	25.2	12.2	39.7°N	215.6°E
Site 422	25°04.425′N	75°33.524′E	6	28.1	−25.6	28.1	−25.6	100.6	6.7	43.5°N	216.4°E
Site 424	25°06.286′N	75°14.343′E	3	163.4	−50.3	163.4	−50.3	20.1	28.2	74.2°N	11.2°E
Mean Lower Bhander SS			6			Tilt-Corrected		119	6.2	46.6°N	215.8°E
Lakheri Ls. (Rajasthan)											
Site 411+	25°50.989′N	76°20.680′E	9	214.7	33.9	208.8	24.5	137.8	4.4	−42.2°N	35°E
Site 412+	25°50.815′N	76°20.729′E	7	23.4	−9.5	25.2	−12.5	37.95	10	49.6°N	215.6°E
Site 426+	25°06.295′N	75°05.482′E	12	30.7	−33.5	17.1	−38.9	22.85	9.3	40.1°N	234.2°E
Site 427	25°06.416′N	75°55.572′E	9	131.5	69.6	208.8	85.1	8.61	18.6	8.5°N	175.3°E
Lakheri Ls. (Rajasthan) Mean			3					74	14.4	44.3°N	222°E
Lakheri Ls. (Son)											
Site 458	24°35.474′N	80°43.292′E	8	346.8	56.6	346.8	56.6	11.67	16.9	50.9°N	343.2°E
Site 467	24°18.581′N	80°46.163′E	5	102.2	23.6	102.2	23.6	99.78	7.7	−11.9°N	77.4°E
Site 468+	24°15.357′N	80°48.272′E	4	62	−35.4	62	−35.4	262.4	5.7	15.4°N	201.1°E
Site 469*	24°17.514′N	80°53.631′E	12	352.0	48.1	352.0	48.1	243	2.8	–	–
Site 470*	24°36.466′N	80°56.551′E	10	348.6	48.1	348.6	48.1	161.7	3.8	–	–
Site 471*	24°36.086′N	80°56.626′E	5	353.1	46.1	353.1	46.1	73	9	–	–
Site 472	24°35.720′N	80°56.242′E	8	315.8	64.3	315.8	64.3	26.23	11	28.8°N	326.1°E
Site 473*	24°33.523′N	80°59.779′E	7	349.2	47.4	349.2	47.4	224	4	–	–
Site 474*	24°33.452′N	80°24.602′E	7	353.4	48.9	353.4	48.9	224	4	–	–
Site 476*	24°33.342′N	81°24.600′E	5	348.8	44.2	348.8	44.2	316	3.4	–	–
Site 477*	24°33.352′N	81°24.568′E	4	356.7	40.6	356.7	40.6	672	3.5	–	–
Site 16+	24°15.9′N	80°48.2′E	3	28.6	−21	32	−21	1500	3	43.0°N	215.4°E
Site 17+	25°15.4′N	80°48.3′E	10	54	−9.8	52	−13	24.3	10	30.3°N	195.5°E
Mean Component B*			6	351.7	46.2			506	2.7	–	–
Mean Component A+			3					25	25.1	−29.7°N	23.3
Mean Raj+Son A+			6				TC	25.3	13.8	−37.5°N	31.8°E
Rewa Ss.											
Site 437	26°59.129′N	77°36.778′E	4	348.8	48.3	10.3	46.4	599.3	3.8	60.6°N	18.8°E
Site 456	24°40.590′N	80°12.982′E	–	–	–	–	–	–	–	–	–
Site 475	24°58.203′N	81°41.043′E	5	343.1	−44.2	339.2	−38.1	279.8	4.6	−60.5°N	42.2°E
Site 461	24°12.613′N	80°48.220′E	4	14.5	−13.5	16.7	−14.8	18.83	21.7	54.3°N	231.6°E
Site 462	24°11.176′N	80°48.778′E	7	15.4	−21	17.4	−29.7	20.27	13.7	46.4°N	236.1°E
Site 466	24°12.613′N	80°48.220′E	4	14.3	−6.4	15.5	−11.2	12.97	26.5	56.5°N	232°E
Site 481	24°21.823′N	81°20.637′E	3	19.7	12.3	18.3	12.1	13.33	35.2	64.7°N	214.3°E
Site 482	24°22.035′N	81°20.288′E	4	28.3	−14.7	29.9	−13.7	30.31	17	47.7°N	214.6°E
Site 19	24°12.5′N	80°48.2′E	5	224	5	222	16	22	16.7	−37.8°N	23.9°E
Site 33	24°11.2′N	80°48.8′E	21	21	20	19.2	−8	20	6.6	56.2°N	224.7°E
Site 41	24°16.9′N	80°42.9′E	7	55	7	60	−29.1	27	11.7	19.2°N	198.6°E
Site 42	24°16.9′N	80°42.8′E	9	211	9	221.3	37.3	27	10.1	−29.9°N	35.6°E
Site 43	24°29.8′N	81°32.6′E	6	26	6	28	−18.4	47	9.9	46.6°N	219.1°E
Site 45	24°27.7′N	81°35.8′E	2	53	2	50	−10.3	–	–	33°N	196.1°E
Mean Rewa SS		Sites	11				Tilt-Corrected	24	9.5	45.6°N	215.2°E
Mean Normal Polarity		Sites	11				Tilt-Corrected	52.7	6.4°	−45.7°N	34.4°E
Mean Reverse Polarity		Sites	23				Tilt-Corrected	27.8	5.8°	43.1°N	213.8°E
Mean Overall			34				Tilt-Corrected	33	4.3°	44.0°N	214.0°E

N: number of samples used to calculate mean; GDec: *In situ* declination, GInc: *In situ* inclination; SDec: tilt-corrected declination; SInc: tilt-corrected inclination; κ: kappa precision parameter; α_{95}: 95% confidence angle about the mean direction; Pole Lat: paleomagnetic pole latitude; Pole Long: Paleomagnetic pole longitude.

to be avoided. Raw isotopic data obtained from the LA-MC-ICP-MS were imported into a Microsoft Excel® spreadsheet where they were corrected for instrumental drift and mass bias. Data reduction is based on the FC-1 (Duluth Gabbro) zircon standard, dated at 1099.3 ± 0.3 Ma ($^{207}Pb/^{206}Pb = 0.0762$, $^{207}Pb/^{235}U = 1.9428$ and $^{206}Pb/^{238}U = 0.1850$) by Paces and Miller (1993), as well as being dated more recently by Black et al. (2003) at 1099.0 ± 0.7 and 1099.1 ± 0.5 Ma. Common Pb correction was applied in the above Microsoft Excel® spreadsheet as well, using the $^{207}Pb/^{206}Pb$ correction outlined in Williams (1998). Isotopic ages and degrees of concordance were calculated and concordia plots were generated using Isoplot/Ex plotting software Version 2.4 (Ludwig, 2000).

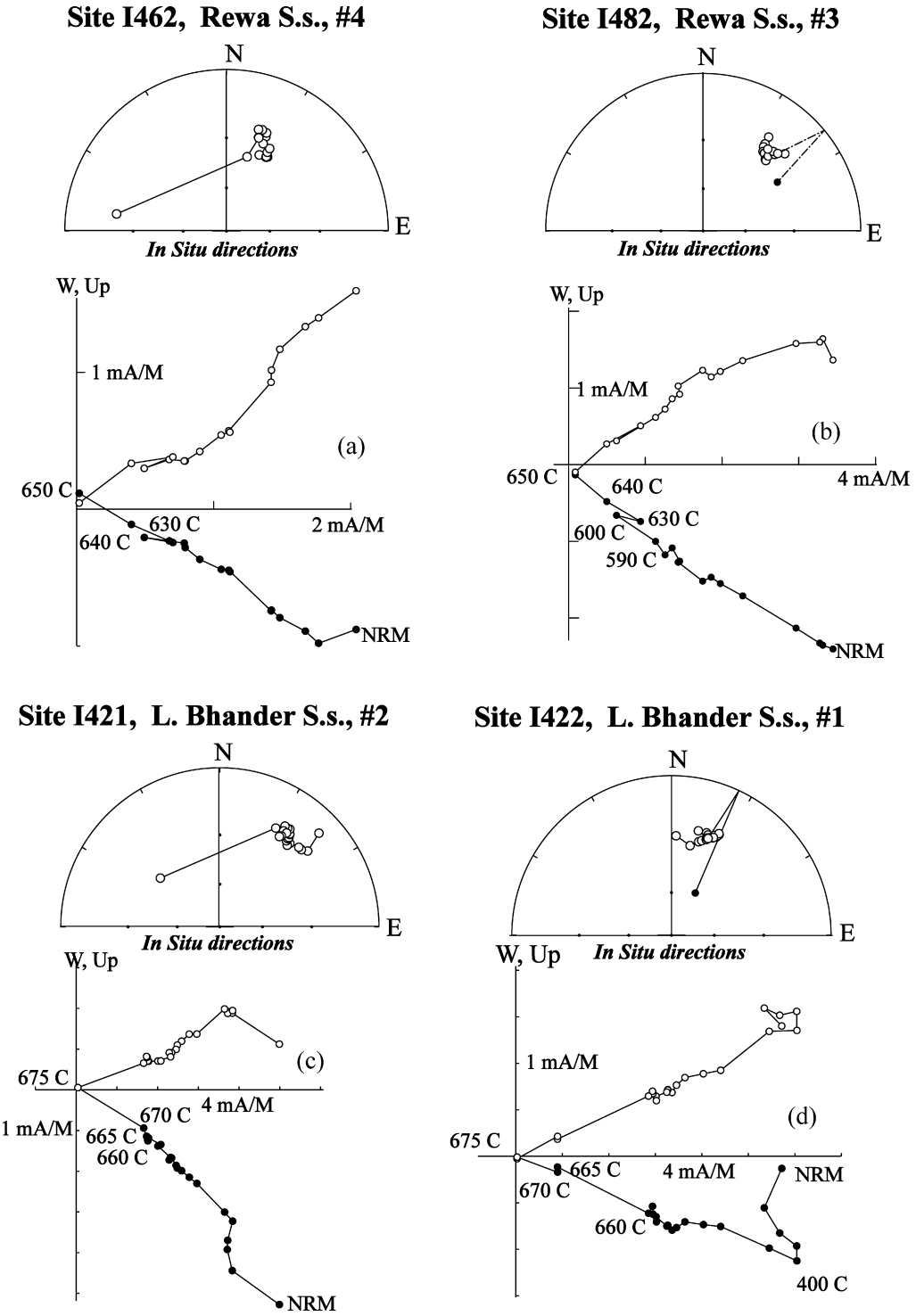

Fig. 4. *In situ* demagnetization plots for (a) Rewa sandstone at site 462 (Son Valley section) and (b) Rewa sandstone from site 482 (Son Valley section) and (c) L. Bhander sandstone from site 421 (Rajasthan) and (d) L. Bhander sandstone from site 422 (Rajasthan). Open/closed circles in the stereoplots represent upward/downward directed vectors and open/closed circles in the Zijderveld plots represent vertical/horizontal projections.

4. Results

4.1. Paleomagnetism

Paleomagnetic results for the Bhander and Rewa Groups correlate well with the previous research and are summarized in Table 2. Generally speaking, demagnetization behaviors showed univectorial decay to the origin and low-temperature demagnetization had little effect on direction/remnant intensity. Hematite bearing samples identified in rock magnetic tests (Section 4.2) and pilot runs showed mostly univectorial demagnetization paths under thermal demagnetization with little evidence of low temperature overprints. Thermal treatments for the sandstones were favored, as hematite appeared to be the primary carrier seen in pilot runs and

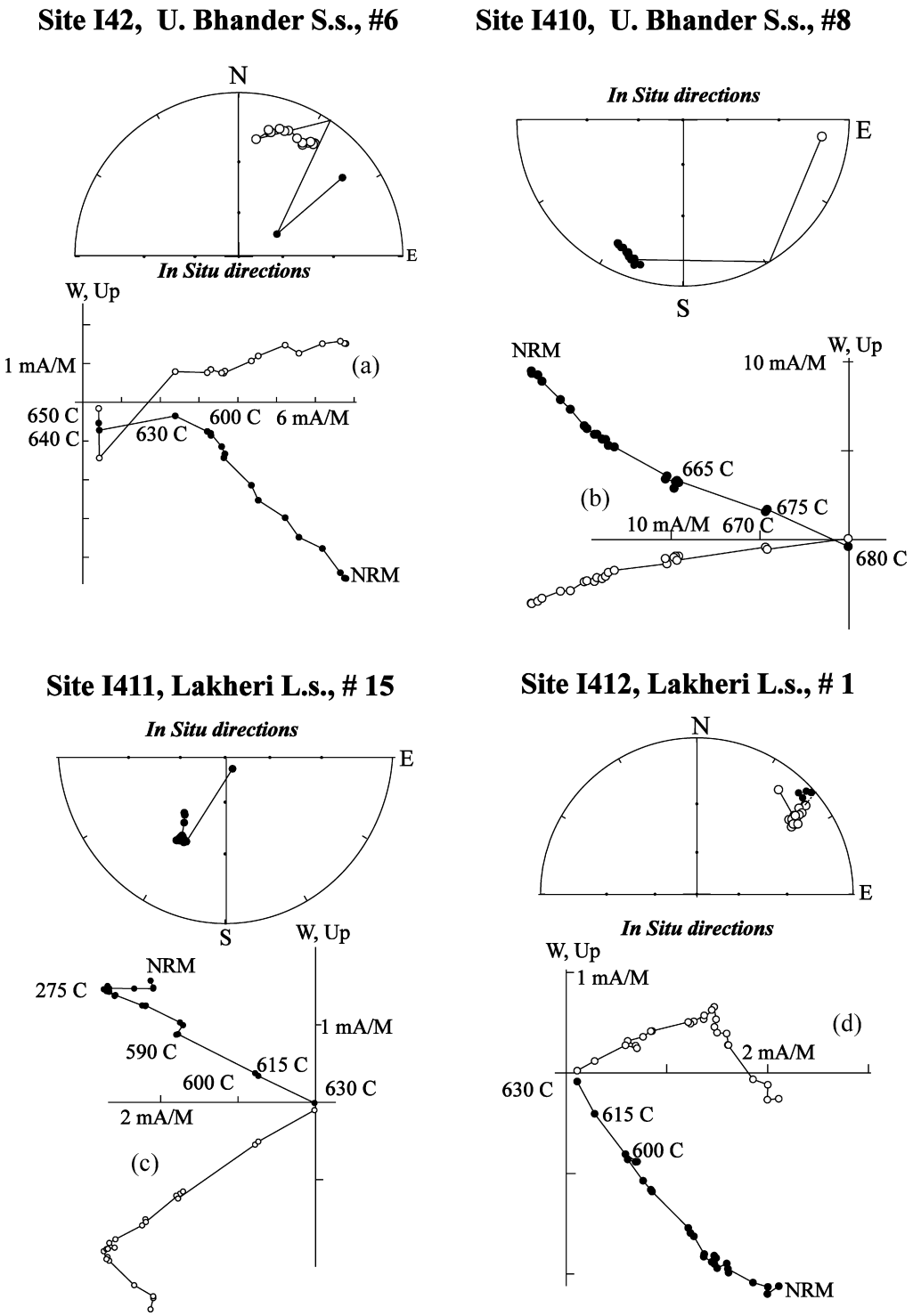

Fig. 5. *In situ* demagnetization plots for (a) Upper Bhander sandstone at site 42 (Rajasthan section) and (b) Upper Bhander sandstone from site 410 (Rajasthan section) and (c) Lakheri limestone from site 411 (Rajasthan) and (d) Upper Bhander sandstone from site 412 (Rajasthan). Open/closed circles in the stereoplots represent upward/downward directed vectors and open/closed circles in the Zijderveld plots represent vertical/horizontal projections.

rock magnetic tests (see Curie temperature results, intensity decay plots and IRM acquisition curves). For reference purposes, (+) inclinations are referred to as 'normal' and (−) inclinations are 'reverse' in this paper.

Fourteen sites were sampled from the Rewa sandstone, and eleven yielded consistent directions (Table 2). Fig. 4a and b shows the demagnetization behaviors for two typical specimens of the tan and purple Rewa sandstone sites. The average NRM intensity for the Rewa sandstones was 2.80 mA/m. Tilt corrected paleomagnetic directions for the eleven Rewa sites range between $D = 15.5–60^\circ$ and $I = -8^\circ$ to -29.1° with two 'normal' magnetized sites at $D = 222^\circ$, $I = 16^\circ$ and $D = 221.3^\circ$, $I = 37.3^\circ$. The tilt corrected directions yield a 'reverse' paleomagnetic pole of 48.2°N and 216.7°E ($N = 9$ sites, $\kappa = 23$, A95 = 11°), and a 'normal' pole at 34°S and 30.1°E ($N = 2$ sites). The overall mean paleomagnetic pole calculated by combining normal and reverse directions is 45.6°N, 215.2°E ($\kappa = 24$, A95 = 9.5°).

The Lower Bhander sandstone consisted mainly of tan to reddish fine grain sandstones, with NRM intensities averaging 3.76 mA/m. Six of the eight sampled sites in the Lower Bhander sandstone show simple demagnetization behaviors (Fig. 4c and d) and exhibit only one polarity with tilt corrected directions ranging between $D = 19.2–31^\circ$ and $I = -7.6^\circ$ to -30.1°. The tilt-corrected paleomagnetic pole derived from the lower Bhander sandstone lies at 46.6°N, 215.8°E ($\kappa = 119$; A95 = 6.2°).

The red Upper Bhander sandstone and Sirbu shale exhibit primarily 'normal' directions compared to those observed in the Lower Bhander (Fig. 5a and b). Eleven of the 12 sampled sites in the Upper Bhander had an average NRM intensity of 11.09 mA/m and yield tilt corrected 'normal' directions ranging between $D = 201.6–227^\circ$ and $I = 2–33.9^\circ$ with three 'reverse' sites characterized by inverted directions at $D = 32–51^\circ$, $I = -10.8^\circ$ to -38°. The combined paleomagnetic pole generated from the eleven upper Bhander and Sirbu shale sites plots at 44.4° S, 33.2°E ($\kappa = 37$; A95 = 7.6°).

The magnetization in the Lakheri–Bhander limestone samples was less stable than the other stratigraphic units sampled. Sites in the Lhakheri limestones from the Rajasthan region yielded 3 sites (1 normal, 2 reverse) with directions similar to those mentioned above. The fourth site, from a complex fold, yielded a steep component that was poorly grouped (Table 2) and is not considered further in our analysis. Ten Son Valley sites of gray to black limestone yielded weak NRM intensities (1.722–0.278 mA/m) and demagnetized at relatively low temperatures (≤450 °C). In particular, seven of the sites within the Lakheri limestones gave consistent directions with a mean *in situ* declination = 351.7° and inclination of 46.2° ($\kappa = 506$, $\alpha_{95} = 2.7^\circ$). This direction is indistinguishable from the time averaged field direction calculated for these sites ($D = 0$, $I = +43^\circ$). We refer to this as the B-direction and attribute them to a viscous remagnetization of recent origin (Table 2).

Three Son Valley Lakheri sites, 468, S16 and S17, did yield directions consistent with the majority of the Upper Vindhyan sites and relatively simple demagnetizations (Fig. 5c and d). The tilt corrected directions for these consistent Son Valley sites, as well as the Rajasthan Lakheri sites, range between $D = 25.2–62^\circ$ and $I = -10^\circ$ to -35.4°, with one 'normal' site with $D = 208.8^\circ$, $I = 24.5^\circ$. The three sites from Rajasthan and three from the Son Valley lobe show similar directions and appear to confirm the broad stratigraphic correlation drawn between the Upper Vindhyan carbonate units on either side of the basin. A combined paleomagnetic pole from these six sites falls at 37.5°S, 31.8°E ($\kappa = 25.3$, A95 = 13.8°).

Table 2 summarizes the site mean paleomagnetic directions from this study. As seen by the site mean VGP's (Fig. 6a–d) and summarized in a generalized magnetostratigraphic column (Fig. 7), the data suggest the presence of at least eleven magnetic field reversals during the deposition of the Upper Vindhyan sediments. The mean 'normal' paleomagnetic pole is derived from eleven sites and falls at 45.7°S, 34.4°E ($\kappa = 52.7$; A95 = 6.4°; Fig. 8a). The mean 'reverse' paleomagnetic pole is derived from 23 sites and falls at 43.1°N, 213.8°E ($\kappa = 27.8$; A95 = 5.8°; Fig. 8b). A McFadden and McElhinny (1990) reversal test performed on the site mean directions yields a 'B' classification ($\gamma_c = 8.7^\circ$) with the angular difference between the normal and reverse directions of 2.6°. Fold tests performed on the Upper Vindhyan sites proved inconclusive. This is most likely

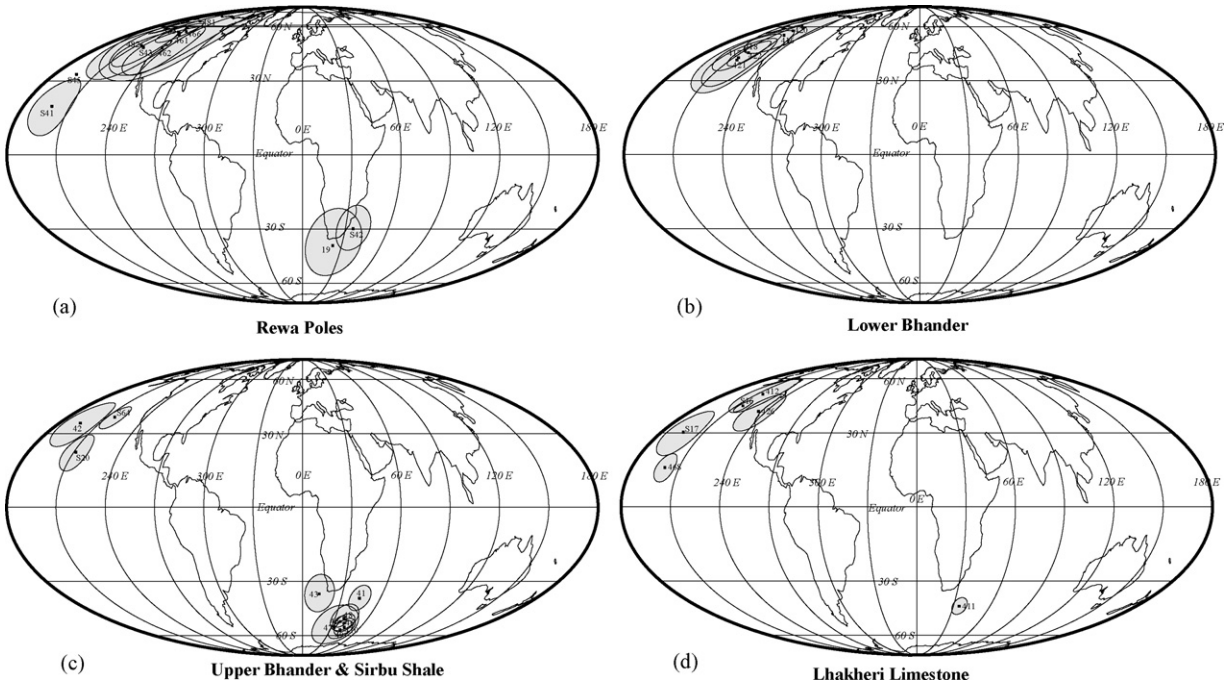

Fig. 6. (a) Virtual geomagnetic poles from the Rewa sandstone; (b) virtual geomagnetic poles from the Lower Bhander sandstone; (c) virtual geomagnetic poles from the Upper Bhander and Sirbu shale and (d) virtual geomagnetic poles from the Lakheri limestone sites. Data are keyed to Table 2. S-prefix sites were collected in 2002 and 4-prefix sites were collected during 2004–2005 field season.

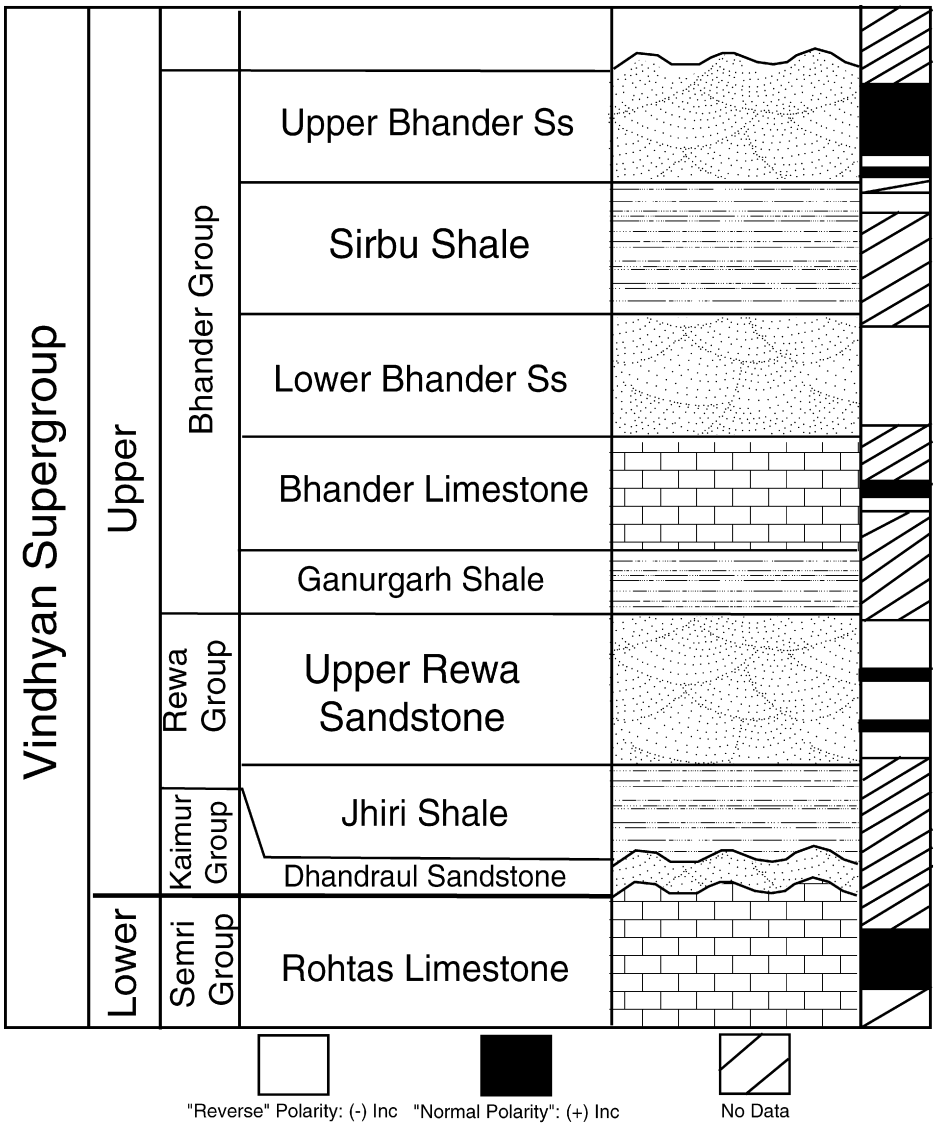

Fig. 7. Generalized polarity stratigraphy for the Upper Vindhyan SuperGroup in this study. Outcrop accessibility limited any detailed measured magnetostratigraphy, but the reversal outlined in this figure is in correct relative stratigraphic order.

due to the low dips and limited deformation seen in the Upper Vindhyan sequence. A comparison between the Upper Vindhyan paleomagnetic directions and those of commonly encountered Indian overprints are quite different, as seen in Fig. 9. Although not conclusive, the presence of geomagnetic field reversals and the directional differences between the Bhander–Rewa direction and common Indian overprints suggests a primary magnetization.

4.2. Rock magnetic tests

The thermal demagnetization behavior of the Bhander and Rewa sandstones are generally consistent with hematite as a primary carrier mineral for most sites. High unblocking temperatures, typically between 630 and 680 °C, are indicative of hematite and are seen in the majority of the sandstone samples. Intensity decay plots (Fig. 10a and b) show little evidence of magnetite based remanence being lost in the 500–580 °C range, providing further evidence that hematite is the primary carrier. The carrier mineralogy is further defined by rock magnetic tests. Curie temperature runs for many sandstone samples show a sharp loss of susceptibility at temperature ranges characteristic of hematite between 613.6 and 700.9 °C. Site 466, tan sandstone from the Rewa Group, shows a heating Curie temperature at 700.9 °C and a cooling Curie temperature at 699.6 °C (Fig. 11a). The red sandstones from site 43 and 48 show a drop in heating susceptibility at 670.5 and 683.1 °C respectively, with a cooling Curie temperature at 670.5 and 682.1 °C, respectively (Fig. 11d and e).

Other sandstones show lower Curie temperatures that may be indicative of minor magnetite or impure hematite contributions. For example, site 422, light brown Lower Bhander sandstone, has a heating Curie temperature of 551.5 °C and a cooling Curie temperature of 535.2 °C (Fig. 11c). The intensity decay plot for site 422 (Fig. 10) still shows the main loss of intensity after heating above 600 °C. This may be due to the presence of higher Ti-magnetite and/or Ti-hematite in the sample. The red Bhander–Lakheri limestone sites exhibit different behaviors. Two Rajasthan red-bed limestone sites (I411 and I412) show hematite as a primary carrier. The demagnetization behavior was more complex than the sandstones with remanence being lost by 630 °C. Curie temperature runs on the red limestone from site 412 shows a lower Curie temperature than is seen in the red sandstones noted above with a heating Curie temperature of 613.6 °C and a cooling Curie temperature of 586.8 °C.

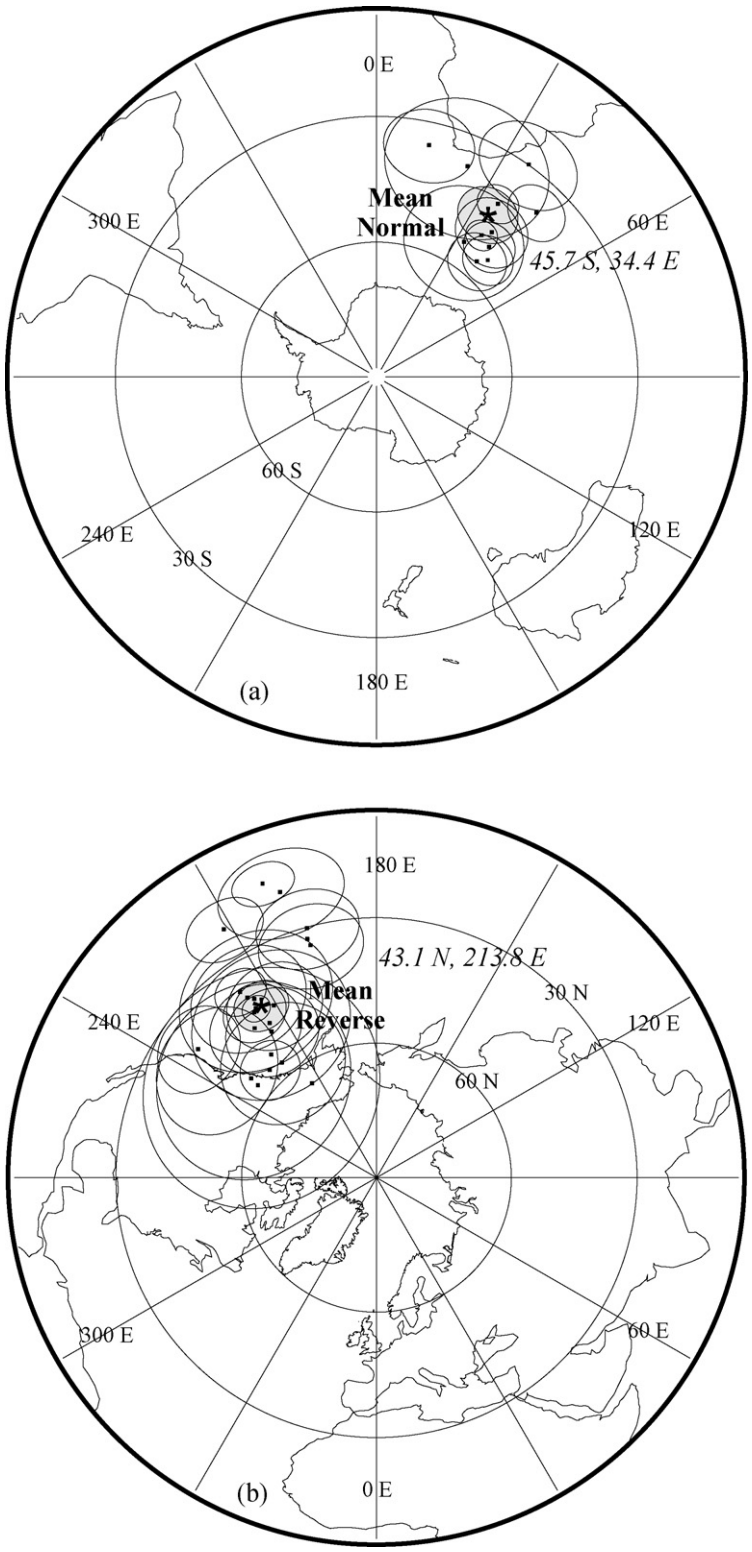

Fig. 8. (a) Summary virtual geomagnetic poles from all 'normal' polarity sites in this study and (b) virtual geomagnetic poles from all 'reverse' polarity sites in this study. Data are keyed to Table 2. The reversal test yields a classification of "B".

IRM acquisition tests for the Upper Bhander, Lower Bhander and Rewa sandstones, as well as the Lakheri limestone (Fig. 12) were also performed on selected samples. Typical curves (Fig. 12a) for the Son Valley black (sites 467 and 473) and gray limestone (site 458) shows saturation by 0.4 T, indicative of magnetite. It is noteworthy, however, that these samples unblocked at low temperatures under thermal demagnetization and carried radically different directions (NW declinations; moderate inclinations- see Table 2) from the units immediately lower and higher in the stratigraphic column. Some samples (see I426, Fig. 12a) showed some evidence of a minor hematite contribution. IRM measurements on the red Upper Bhander sandstones produced the characteristic curve of hematite,

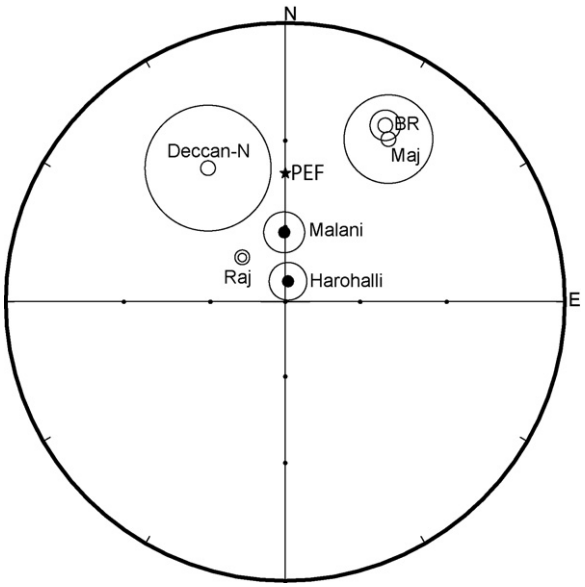

Fig. 9. Bhander, Lakheri and Rewa directions from this study (a), BR: a composite mean from this study and Maj: Majhgawan kimberlite pole compared to Malani igneous province directions (771 Ma) Harohalli dykes directions (previously assumed at 823 Ma); Rajmahal (Raj) traps (180 Ma) and Normal Deccan traps directions (65 Ma). The Upper Vindhyan directions are statistically different from all of these potential overprint directions.

failing to saturate at fields up to 2.0 T (Fig. 12b). The tan and purple sandstones more characteristic of the Lower Bhander and Rewa sandstones (e.g. sites 422 and 466, Fig. 12b) were also dominated by hematite, but included contributions from magnetite as well. This minor contribution can be seen in the sharper saturation seen in the applied fields between 0.05 and 0.2 T (Fig. 12b), but the lack of total saturation until higher applied fields suggests hematite as the main carrier.

4.3. Geochronology

Mineral separation and analysis of separated zircon grains was carried out in accordance with the methods outline in Section 3.2 above. The Rewa Group contains several ash fall and volcaniclastic units; however, these yielded few useful zircon grains for geochronology. Of multiple ash beds sampled, only one yielded a suite of minerals suitable for radiometric dating. Small (~40 μm × 120 μm) sub- to euhedral zircon grains were extracted; however, U–Pb analysis of these grains yielded equivocal results. Most of the grains analyzed showed very discordant dispersions between $^{206}Pb/^{238}U$ and $^{207}Pb/^{235}U$ ages as well as high common Pb. From 23 grains analyzed, only 3 yielded concordant ages. Two grains yield an age of 1555 Ma, and a single grain yielded an age of 1053 Ma. Because of the limited sample size, these results are not considered further.

The detrital zircon sample processed from the Upper Bhander sandstone (sampled from sites 43, 44 and 45, Rajasthan section) yielded numerous datable grains with varying degrees of concordance. One sample set (Undifferentiated U. Bhander) was separated from paleomagnetic sample cores representing sites 43, 44 and 45. The grains were typically small (<250 μm) and mildly to strongly abraded, as is visible in Fig. 13a. Of 210 analyses, 152 grains were within 10% of concordance (Fig. 14a). 1800 Ma zircons form the largest population in the sample. The youngest population peaks at ~1020 Ma. Several other age populations are resolved at 1140, 1260, 1380, 1600 and 1740 Ma. A small population of Archean grains is also present, ranging between 2500 and 2680 Ma.

Two sites of Marwar SuperGroup sandstone (Girbhakar and Sonia sandstones) were similarly processed to extract detrital zircons. The Girbhakar sandstone yielded 75–200 μm sub- to euhedral grains, as well as small euhedral to subhedral zircons with mild abrasion (Fig. 13b); when analyzed, the vast majority (71) of these grains gave results within 5% of concordance (Fig. 14b). The Sonia sandstone yielded 60 smaller, abraded grains with a higher incidence of discordant ages. The age distribution for both sandstones, however, was similar. These analyses yielded a major age peak for the Marwar SuperGroup centered between 800 and 900 Ma ($^{206}Pb/^{238}U$), with trivial occurrences of Meso- and Paleoproterozoic grains (16.4% of grains occurring in a small population ~1000 Ma or single grains between 1100 and 2100 Ma). Also present in the Marwar sample were two concordant ~780 Ma grains. Fig. 15 illustrates the probability density function for the Upper Bhander and Marwar detrital zircon ages, broken down by site (a–f) and shown as a whole (g and h).

5. Discussion

5.1. Age of the Bhander–Rewa: fossil evidence

Previous age determinations derived from the Bhander and Rewa Groups typically are ambiguous and lack consistency. Fossil markers found in the Bhander–Rewa Groups, such as *Chuaria*

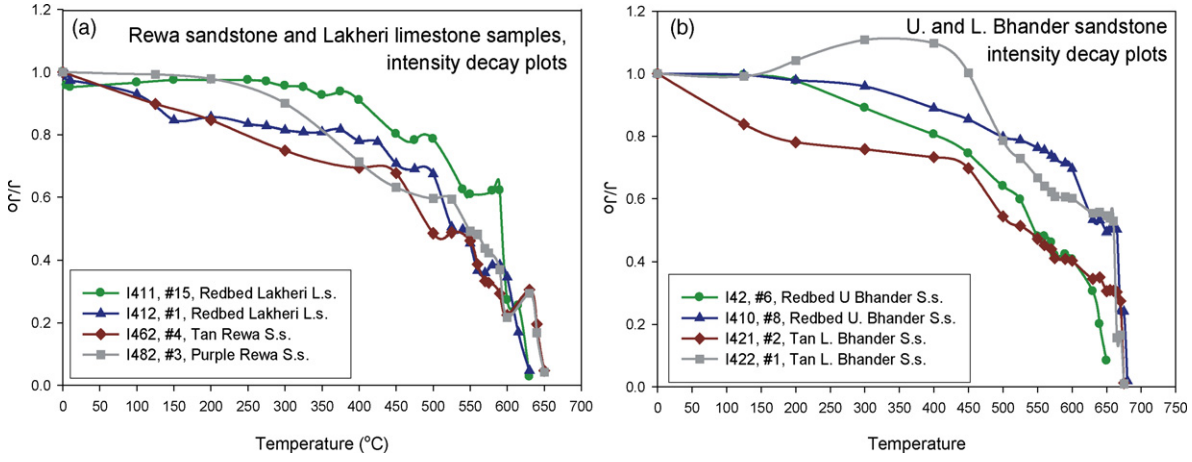

Fig. 10. (a) Intensity decay plots for thermally treated samples of the Rewa sandstone and Lakheri limestone and (b) intensity decay plots for thermally treated samples of Upper and Lower Bhander sandstone.

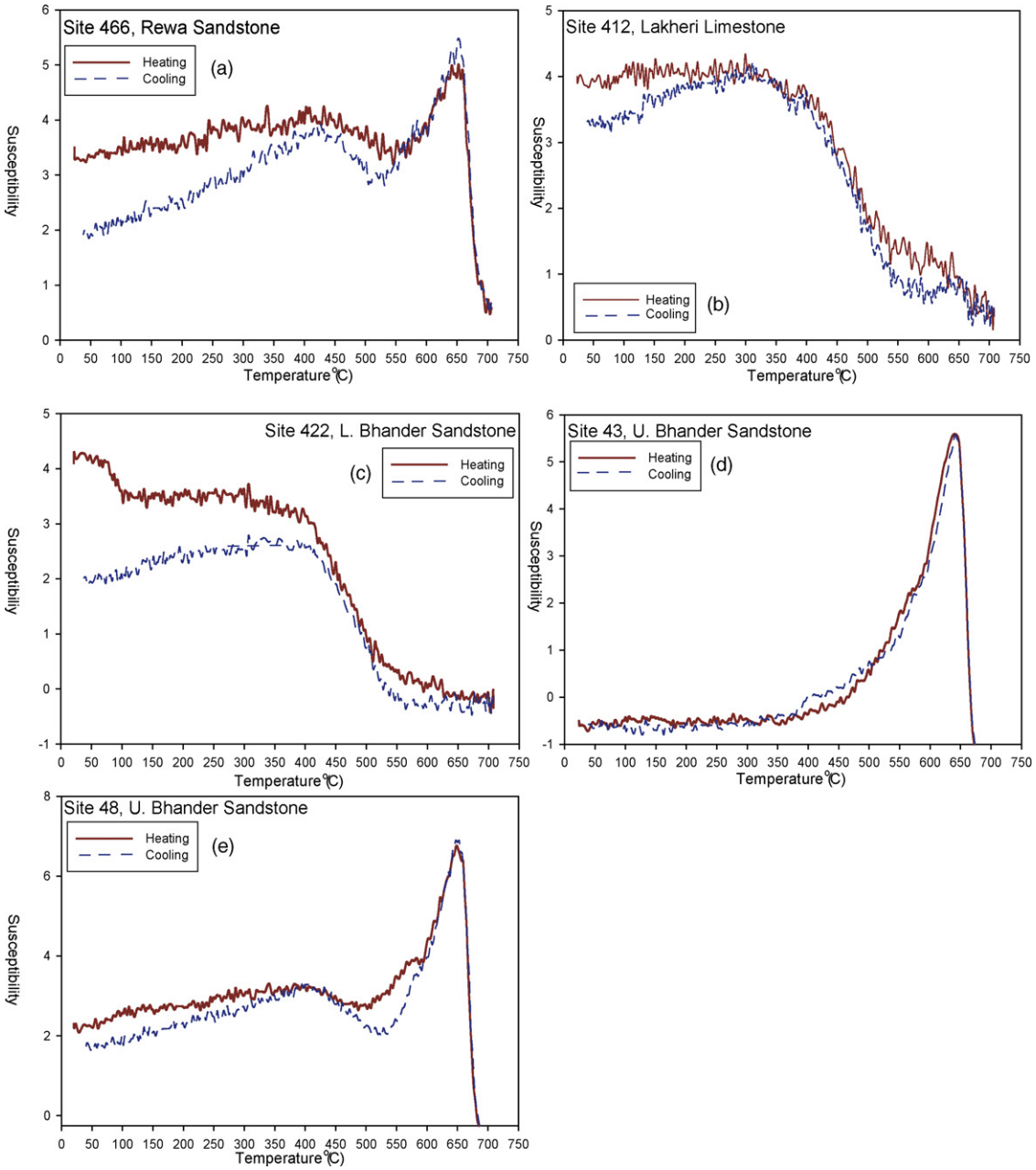

Fig. 11. Curie temperature runs for selected samples in this study (a) tan Rewa sandstone showing a heating Curie temp of 700.9° and a cooling Curie temperature of 699.6 °C; (b) Reddish Lakheri limestone sample with near-reversible behavior and a Curie temperature of ~565 °C and a small contribution from hematite at temperatures >600 °C; (c) Lower Bhander sandstone sample showing a heating Curie temperature of ~552 °C and a slightly lower cooling Curie temperature; (d) Red Upper Bhander sandstone sample showing nearly reversible Curie temperature curves with a Curie temperature of 671 °C; (e) Red Upper Bhander sandstone with nearly reversible curves and a Curie temperature of 683 °C.

and *Tawuia* (Rai et al., 1997; Kumar and Srivastava, 2003) and possible burrows (Chakrabarti, 1990) do not have a narrow enough range or good enough preservation to act as suitable index fossils. De's (2003, 2006) Ediacara-like fossils in the Lakheri–Bhander limestone suggest that the Bhander–Rewa Groups are Ediacaran in age, consistent with some previous assertions. The utility of the Ediacara fauna described by De (2003, 2006) is limited until it is confirmed independently. This confirmation is needed, as illustrated by previous fossil findings in the Vindhyan Basin that have been challenged (Bengtson et al., 2007).

One further possibility to consider with the alleged Ediacara fossils (De, 2003, 2006) is that they may be older than normally considered. Rasmussen et al. (2004) used authigenic xenotime overgrowths on detrital zircon grains to date fossils of an Ediacaran affinity from the Sterling Range Formation, in southwest Australia. Rasmussen et al. (2002a,b) previously dated the formation using detrital zircon and metamorphic monazite between 2.0 and 1.2 Ga. The new ages derived from the xenotime overgrowths indicate that the fossiliferous Sterling Range Formation was deposited prior to 1800 Ma, with a detrital zircon defined maximum age of 2015 Ma (Rasmussen et al., 2004). This suggests that Ediacara-like fossils, or features resembling them, can be found in rocks older than normally defined as Ediacaran age (<635 Ma). More recently, Bengtson et al. (2007) reported "Ediacaran-like' fossils from the Lower Vindhyan and suggested that these represent an indication of previously hidden biodiversity in the Paleo- and Mesoproterozoic.

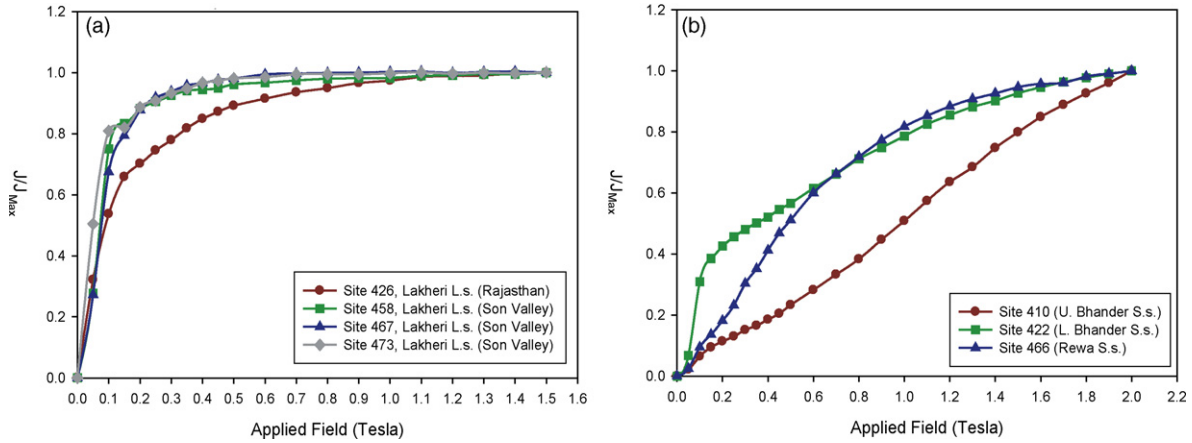

Fig. 12. Selected isothermal remanence acquisition studies of (a) Lakheri and Bhander limestone samples and (b) Upper and Lower Bhander sandstones and a Rewa sandstone.

5.2. Age of the Bhander–Rewa: correlations with global events

Recent attempts to directly date the Lakheri–Bhander limestone resulted in an age estimate of ~750 Ma based on correlations with global $^{87}Sr/^{86}Sr$ ratios for this time (Ray et al., 2002). $^{87}Sr/^{86}Sr$ curves have been developed as a tool for the relative dating of carbonate sequences, as Sr isotopic values are generally believed to be homogenous throughout the ocean. Using $^{87}Sr/^{86}Sr$ values for dating presents several difficulties, however. Values for the Proterozoic, unlike the data from the Phanerozoic, are poorly constrained by reliable ages, as well as suffering from gaps in the record. This method, however, is considered reliable in producing minimum ages for Precambrian carbonates (Ray, 2006). Kumar et al. (2002) observe that the $\delta^{13}C$ values for the Lakheri limestone correlate with the global curve between 700 and 570 Ma. The correlation between $\delta^{13}C$ curves is problematic, especially in the Proterozoic where continuous records are scarce and radiometric age constraints on important markers are rare (Meert, 2007). The negative $\delta^{13}C$ excursions in the Lakheri–Bhander limestone are interpreted by some authors (Kumar et al., 2002) as being associated with Neoproterozoic global glaciations. Kumar et al. (2002) also notes that the Bhander–Lakheri limestone in Rajasthan overlies an intraformational conglomerate he interprets as a tilloid. These data have been used to label the Lakheri limestone unit as a "cap carbonate" associated with "Snowball Earth" Neoproterozoic glaciations. Several problems with this explanation include the equivocal nature of the "glaciogenic tilloids" (Prasad, 1984; Kumar et al., 2002) and the uncertainties associated with the $\delta^{13}C$ excursion documented in the Son Valley Lakheri limestone (Ray et al., 2003; Banerjee et al., 2006). Ray et al. (2003) notes that complications in verifying the $\delta^{13}C$ excursion may be due to the sampling of different horizons of the Lakheri limestone and this assertion was later confirmed by Banerjee et al. (2006).

The Ediacaran-Cambrian interval represents a major period of phosphorite deposition, and is recorded in rock known to be of this age across Australia and south–southeast Asia (Shen et al., 2000; Meert and Lieberman, 2008). The deposits are generally characterized by thick sequences of stromatolitic carbonates overlain by phosphatic black shale and chert (Banerjee and Mazumdar, 1999). Phosphorite deposits that record the transition into the lower Cambrian time outcrop in the Krol and Tal formations of the Lesser Himalayas (Mazumdar and Banerjee, 2001). These deposits have almost identical lithologies to those found in South China, Iran and parts of Arabia, and Banerjee and Mazumdar (1999) use these correlations to place these blocks adjacent to one another at the time. The paleogeographic correlation is also supported by scant paleomagnetic constraints and 'normal' paleolatitudinal constraints on the deposition of evaporites and carbonates (Jiang et al., 2003;

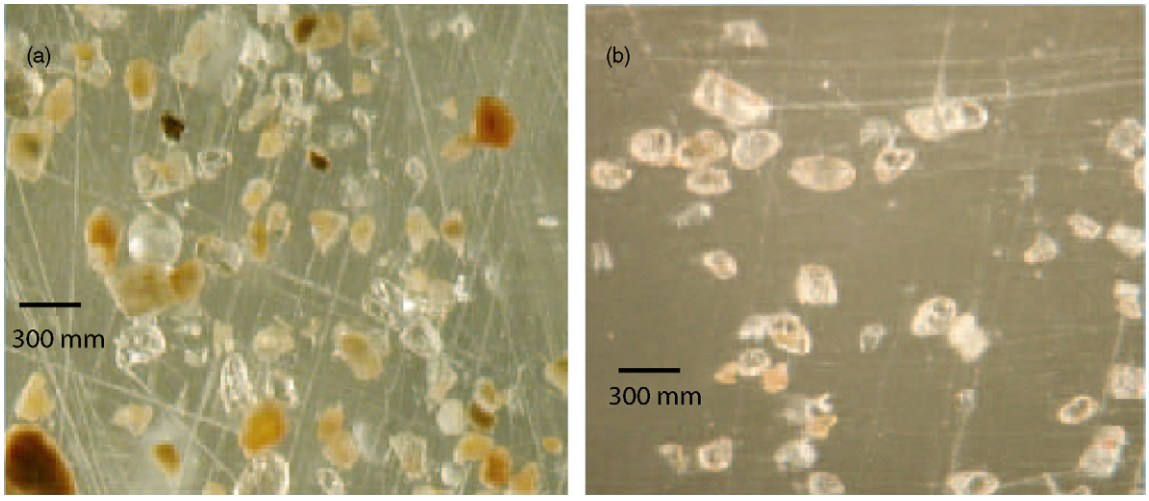

Fig. 13. Photographs of detrital zircons grains analyzed in this study from (a) the Gibhakar sandstone (Marwar SuperGroup) and (b) Upper Bhander Sandstone. Scale bar length is 300 μm.

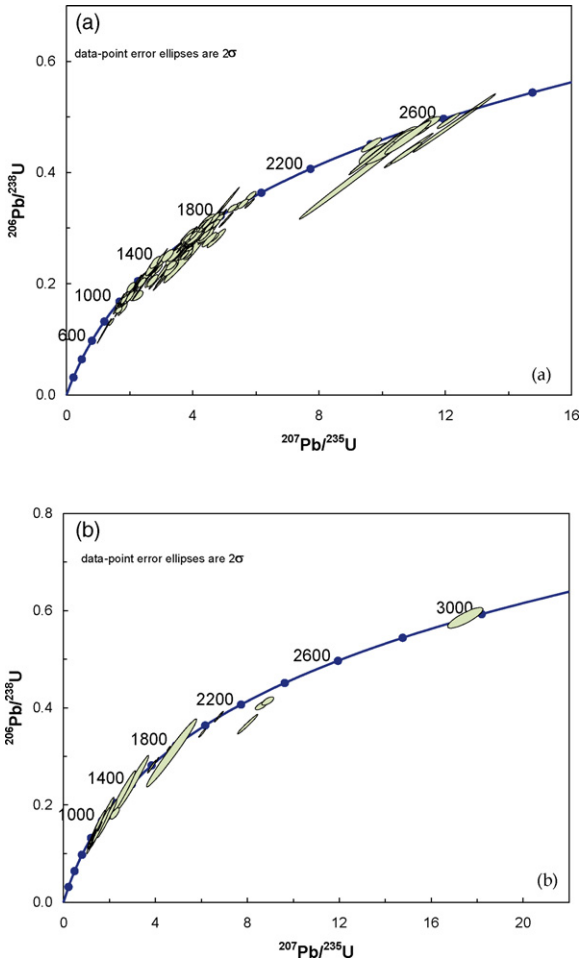

Fig. 14. Concordia plots showing (a) Upper Bhander sandstone zircon grains from sites 43, 44 and 45 in Rajasthan (n = 152 grains) and (b) concordia plots for zircon grains obtained from the Marwar sandstones (n = 118).

Pradhan et al., in press). This discussion becomes important when considering the alleged Neoproterozoic–Cambrian age of the Upper Vindhyan Groups. Lithologies of this sort, and indeed any phosphatic horizons are absent in the upper Vindhyanchal Basin. This absence is noteworthy, considering the regional extent of phosphorites observed by Banerjee and Mazumdar (1999) and the global scale of the phosphate event in the oceans of the time (Meert and Lieberman, 2008).

5.3. Age of the Bhander–Rewa: Paleomagnetic evidence

The Majhgawan intrusion into the Kaimur Group provides an important reference as a cross cutting intrusion at 1073.5 ± 13.7 Ma. The VGP generated from the Majhgawan kimberlite, the Harohalli dykes paleomagnetic pole, and the paleomagnetic pole from the Malani Igneous province provide the best temporally constrained paleomagnetic information covering the suspected period of deposition for the Bhander and Rewa Groups. The comparison of the Bhander–Rewa poles to those from the well dated Majhgawan and Malani sties, however, provides an interesting conundrum. The Bhander and Rewa poles of Athavale et al. (1972), Klootwijk (1973), McElhinny et al. (1978) and this study all plot very closely to the Majhgawan VGPs of Miller and Hargraves (1994) and Gregory et al. (2006) as illustrated in Fig. 16. In contrast, the Malani pole plots far from both the Majhgawan and Bhander–Rewa poles as seen graphically in Fig. 16.

This observation leads to a remarkable interpretation. Although some age estimates on the Bhander and Rewa Group suggest a ~750 Ma age, there is no similarity between the Bhander–Rewa poles and the well constrained Malani Igneous province pole (Gregory et al., submitted for publication; Torsvik et al., 2001a,b). This suggests that the Upper Vindhyan is not, in fact, of a similar age to the Malani Igneous province as implied by the Sr-data of Ray et al. (2003). This dissimilarity may be due to several factors. The possibility of a remagnetization of the Upper Vindhyan units and the Majhgawan kimberlite would explain the apparent similarities between these poles to each other, as well as the apparent correlation they share with the Cambrian APW path with Gondwana. Such a remagnetization event would likely have affected a wider area of India including the Malani Igneous Province and Harohalli dyke swarm (Pradhan et al., in press; Halls et al., 2007). However, the Malani Igneous province and Harohalli dykes paleomagnetic directions (Torsvik et al., 2001a,b; Radhakrishna and Mathew, 1996) typically are very different from the Neoproterozoic–Cambrian Gondwana poles (547 Ma Sinyai dolerite, 755 Ma Mundine Well dykes, etc) as well as the Upper Vindhyan and Majhgawan kimberlite directions. Halls et al. (2007) noted a northerly and very shallow overprint in the Harohalli dykes (paleomagnetic pole at 76.5° S, 68.8° E; Dharwar craton) that they attributed to a Neoproterozoic overprint associated with final Gondwana assembly. Pradhan et al. (in press) argue the case for an Ediacaran age for the overprint observed in the Harohalli dykes (Fig. 16 pole Hao). A Malani age of remagnetization is therefore highly unlikely, due to the major differences in directions between the Malani Igneous province and the Upper Vindhyan noted above. Additional support for the primary nature of magnetization is found in the presence of at least eleven geomagnetic reversals in the Upper Vindhyan sedimentary units. A third possibility is that the Bhander–Rewa are, in fact, Ediacaran in age and the similarities to the older Majhgawan kimberlite are fortuitous. The final alternative is that the Bhander–Rewa poles are of similar age to the Majhgawan kimberlite and the Vindhyan Basin sedimentation is far older than previous estimates. We discuss these alternatives below.

5.4. Detrital zircon geochronology and provenance

The detrital zircon geochronology conducted in this study offers further clues into the possible age of the Bhander–Rewa sequence. The $^{207}Pb/^{206}Pb$ age distribution yields several noteworthy peaks that can be correlated with regional tectonic and magmatic events. The largest peak recorded in the Upper Bhander sandstone of Rajasthan, at circa 1600 Ma, correlates well with the volcanic activity recorded in the Lower Vindhyan Deonar porcellanite which is precisely dated between 1593 and 1630 Ma (Rasmussen et al., 2002a; Ray et al., 2002). The secondary peak at 1850 Ma seems to correlate with the ages from the Hindoli Group of Deb et al. (2002), and the ~1800 Ma ages possibly relate to Banded Gneiss Complex input (Buick et al., 2006). Zircon ages between 1400 and 1100 Ma may correlate with events in the Delhi Fold belt (Biju-Sekhar et al., 2000; Deb et al., 2001), and/or volcanic activity related to ash fall deposits in the Rewa Group. The youngest population in the Upper Bhander sandstone at about 1020 Ma correlates well with volcanic activity described by Patranabis-Deb et al. (2007) from the Sukhda and Sapos tuffs (uppermost section of the Chattisgarh Basin), and may help constrain a maximum age of deposition for the Upper Bhander sandstone. Further constraints may be provided by considering a potential source not represented in the detrital zircon provenance of the Upper Bhander sandstone. The detrital zircon data observed in our population also matches several of the populations from rocks to the NW of the Rajasthan section of the

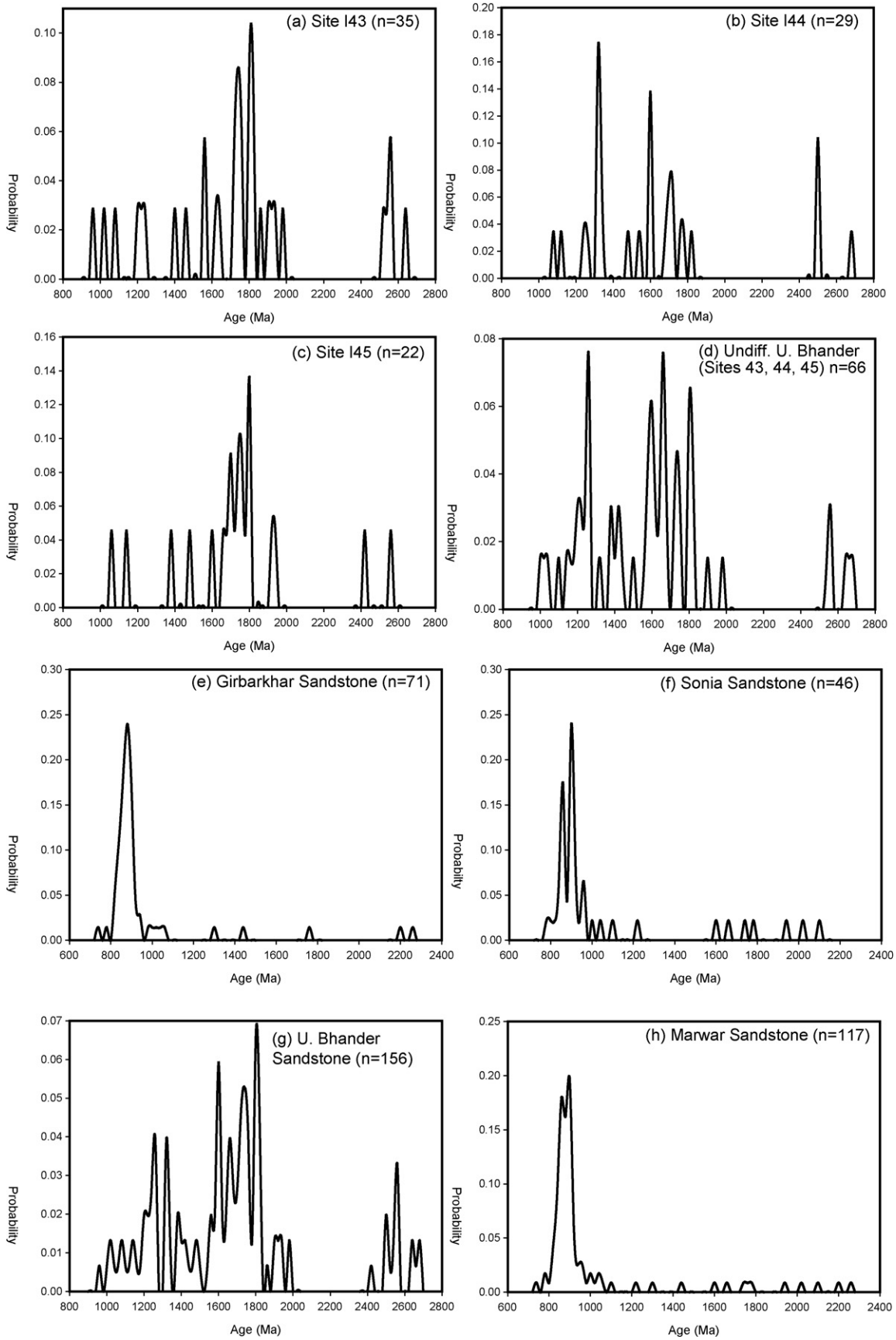

Fig. 15. Detrital zircon probability functions by site for the Upper Bhander sandstones of Rajasthan and the Marwar sandstones. These units have been correlated in the past (Heron, 1932, 1936; Pascoe, 1959) but clearly show a different provenance. (a) Bhander sandstone site 43; (b) Bhander sandstone site 44; (c) Bhander sandstone site 45; (d) Undifferentiated samples from the Bhander sandstone at sites I43, I44 and I45; (e) Girbarkhar sandstone (Marwar) and (f) Sonia sandstone (Marwar).

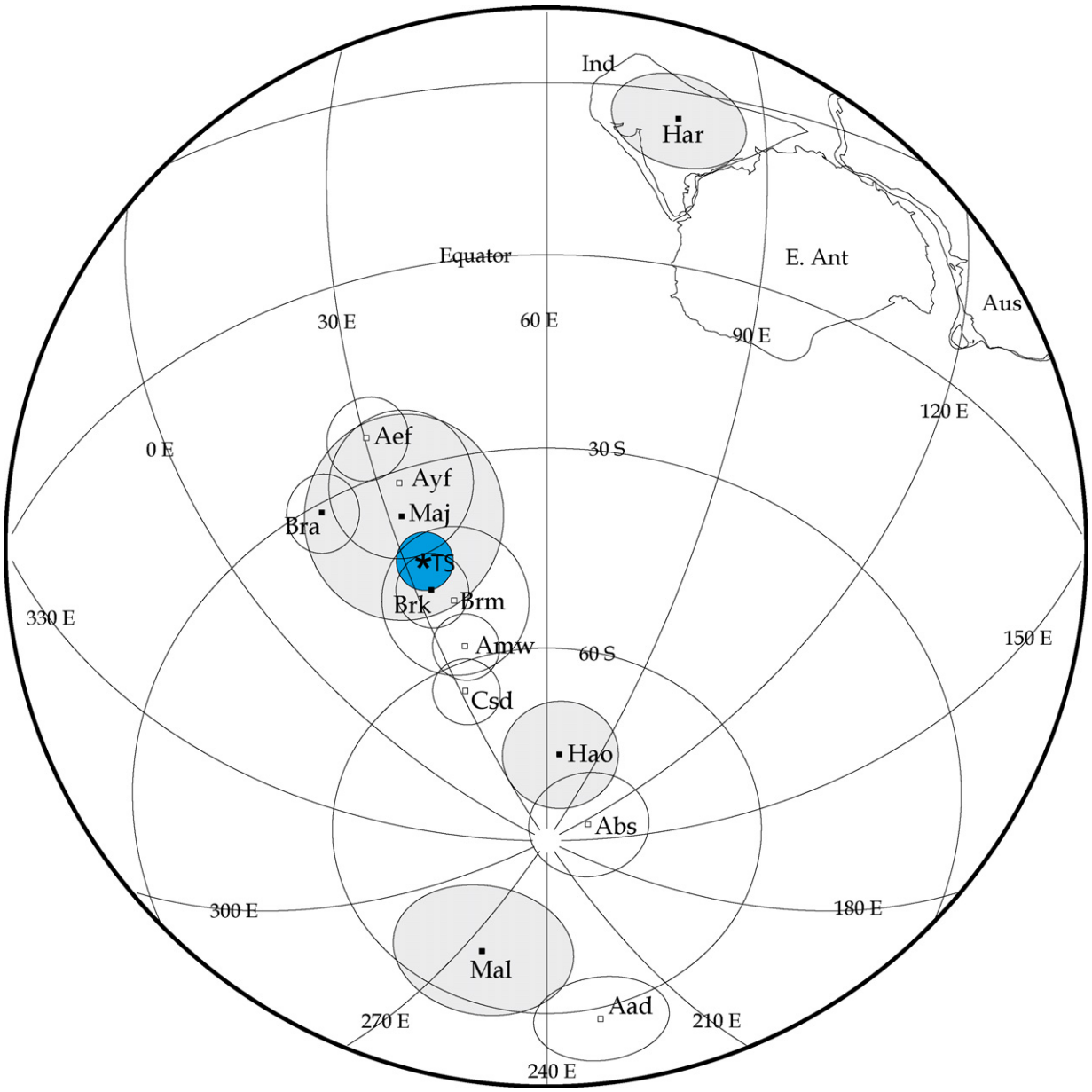

Fig. 16. Paleomagnetic poles from Indian, Australian and Africa given in Table 3. Indian poles are shaded in light grey, Australian and African poles are unshaded. Pole abbreviations are listed in Table 3.

Vindhyan Basin (near Ajmer Fig. 2a) outlined in Fareeduddin and Kroner (1998).

Gregory et al. (submitted for publication) presented a recent U–Pb zircon date from the Malani rhyolite, yielding an age of 771 ± 5 Ma an age consistent with those reported only as 'personal communication' in earlier publications (Torsvik et al., 2001a). Additional geochronologic work on early (and pre-Malani) igneous activity in Rajasthan yielded concordant ages of 786.4 ± 2.8 and 827.0 ± 4.4 Ma (Meert et al., 2008). Together with geochronologic data from the Seychelles (Torsvik et al., 2001b) these data suggest that Malani/pre-Malani magmatism stretched from at least 750–827 Ma. These ages are significant because grains of this age are completely absent from the detrital grains analyzed from the Rajasthan Upper Bhander sandstone. The Malani igneous province, having an area of 54,000 km^2 and a position proximal to the modern position of the Vindhyan Basin, would likely have been contributing sediment (including detrital zircon) to the Bhander sandstones. The absence of Malani age zircon may be due to several factors: (a) The Great Boundary Fault (GBF) acted as a topographic divide during the time of Vindhyan sedimentation, keeping Malani sediments from reaching the basin, (b) The GBF represents a suture after Bhander deposition, or (c) the Bhander sandstone, and hence the remainder of the upper Vindhyan sequence, is far older than the Malani Igneous Province.

The first possibility is difficult to evaluate as a great deal of uncertainty exists about the nature of the GBF. The presence of zircon similar in age to the Hindoli Group (Deb et al., 2002) and Delhi–Aravalli orogen (Fareeduddin and Kroner, 1998; Chakraborty, 2006) that both lie across the GBF in the direction of the Malani province suggests that the fault itself did not inhibit the transport of sediment. The age of the GBF is debatable; however, Verma (1996) states that the GBF is a pre-Vindhyan feature, formed initially as a normal fault that has been reactivated numerous times in geologic history. Prasad and Rao (2006) support the pre-Vindhyan origin of

the GBF when they note the presence of Vindhyan sediments only to the east of the fault trace. Folding of Vindhyan sedimentary units in the vicinity of the GBF trace suggest that it was active during their deposition. The area to the west of the GBF may have been a positive relief feature during the deposition of the Semri Group, suggested by the presence of conglomerates in unspecified horizons (Verma, 1996). Sedimentological studies of the Upper Bhander sandstones provide evidence that low elevation sources provided sediment to the basin. This conclusion is supported by the general lack of unstable minerals and predominance of mature quartz grains in the sandstones (Bose et al., 2001). Collectively, these data are consistent with the notion that sediment could cross the GBF to be deposited in the Vindhyanchal Basin.

The second option is improbable, due to the lack of geologic evidence indicative of a suture zone (e.g., ophiolites, pervasive deformation of the Rajasthan section of the basin, etc). The Vindhyanchal Basin, as suggested by several authors (e.g. Chaudhuri et al., 1999; Bose et al., 2001) notes the limited deformation and stable shelf character of the Upper Vindhyan Groups. Deb et al. (2001) dated igneous rocks representing an arc across the GBF from the Vindhyanchal Basin, and finds that most were emplaced between 987 ± 6.4 and $836 + 7/-5$ Ma. The Malani Igneous province was also erupted/intruded into this region as well as the older (>1700 Ma) Delhi SuperGroup (Deb et al., 2001). The similarity to detrital and metamorphic zircon populations found to the NW of the Vindhyanchal Basin (and to the west of the GBF) also supports our view that the GBF was not a physiographic barrier to deposition of Upper Vindhyan rocks (Fareeduddin and Kroner, 1998).

The third option is quite plausible and is less subject to paleogeographic uncertainties. The absence of any zircons younger than ~1000 Ma in the Upper Bhander sandstone is explained by the >1000 Ma age of the sediments, without the need to resort to complicated paleogeographies and highlands not seen in the sedimentary record. This allows for an age bracket to be inferred for the Upper Bhander sandstone, between 771 Ma (Malani age) and ~1070 Ma (youngest detrital zircon ages, Fig. 15g). Further support for this reasoning is seen in the Marwar SuperGroup detrital zircon ages. The Marwar is thought to be Neoproterozoic–Cambrian based on fossil evidence (Raghav et al., 2005). Detrital zircon grains analyzed from the Girbarkhar and Sonia sandstone show a probability density function distinct from the Upper Bhander sandstone (Fig. 15h). The dominant age population for the Marwar samples peaks sharply in the 840–920 Ma range, a population completely absent in the Upper Bhander. Furthermore, the Marwar grains show a small population of Malani age zircons, again totally absent in the Upper Bhander sandstone. The source for the main 840–920 Ma age peak in the Marwar detrital zircon dataset remains unknown with any certainty, but may be related to igneous events in the South China craton, juvenile crust formed in the Arabian–Nubian shield or igneous rocks emplaced along the western margin of the Delhi–Aravalli fold belt (Deb et al., 2001). The placement of South China adjacent to India during the Neoproterozoic is proposed by Jiang et al. (2003), and Xiao et al. (2007) has recently published U–Pb zircon ages on subduction related igneous activity of this age. Younger detrital zircon ages may be locally derived from granitic magmatic activity (e.g. Erinpura granite) in the accreted arc terrane dated at 840–820 Ma (Deb et al., 2001).

The zircon U–Pb ages Patranabis-Deb et al. (2007) published from the Sukhda and Sapos tuff units provide further support for an adjustment to the age of the Upper Vindhyan sediments. The tuffs were emplaced in the uppermost section of the Chattisgarh Basin, and SHRIMP analysis of zircon separated from these units yields ages of 990, 1015, and 1020 Ma (Patranabis-Deb et al., 2007). These ages are significant, as the Purana Basins of India are reliably thought to be related in age and origin (Chaudhuri et al., 1999). This allows for age determinations for one basin to be applied to the other sister basins across the Indian subcontinent, and offers additional support to the detrital zircon data presented above.

5.5. Paleomagnetic implications of an old (ca. 1000 Ma) Upper Vindhyan Sequence

A simple explanation for the data discussed above may be that the Bhander and Rewa Groups are only marginally younger than the Majhgawan kimberlite. If true, this allows for the Bhander and Rewa poles to be compared to other, ca. 1000–1070 Ma paleomagnetic poles from East Gondwana cratons. Paleomagnetic data from East Antarctica, a major East Gondwana element, are scarce and poorly constrained by reliable geochronology. In contrast, Australia, the other element critical to East Gondwana reconstructions, provides several well dated paleomagnetic poles of the appropriate age generated from mafic intrusions found in the western cratons. Schmidt et al. (2006) recently published a paleomagnetic pole, located at 2.8°N, 84.4°E and dated at ~1070 Ma, from the Alcurra Dyke (Aad) swarm of the Australian Musgrave block. When rotated into India co-ordinates (India fixed; modified from the Africa fixed Gondwana configuration of Norton and Sclater, 1979; see Table 3 for Euler poles) this paleomagnetic pole plots distant from the Majhgawan kimberlite VGP (Maj) or the Upper Vindhyan (TS) paleomagnetic pole as shown in Fig. 16. There is, however, some question about the tilt correction for dyke orientation in that study which may impact any comparisons. The high quality Bangamall Basin (Abs) sill pole at 33.8°N, 95°E, dated at 1070 ± 6 Ma (Wingate et al., 2002), is distinct from the Bhander–Rewa and Majhgawan paleomagnetic poles when similarly rotated into a fixed India position. Fig. 16 shows the positions of these Australian paleomagnetic poles when rotated into India co-ordinates. Traditional reconstructions (e.g. Dalziel, 1997) typically place India adjacent to Antarctica and Australia as part of a coherent East Gondwana. If India and Australia were adjacent, attached cratons at 1.0 Ga, then these poles should lie much closer together. The paleomagnetic data discussed above, however, seem to support models of a separated East Gondwana at the Meso- to Neoproterozoic boundary (e.g. Meert et al., 1995; Powell and Pisarevsky, 2002; Meert, 2003; Meert and Lieberman, 2008). Fig. 17 shows reconstructions for India at ~1050 Ma, using the Bhander–Rewa paleomagnetic pole discussed above and comparing it to the positions of other paleomagnetically constrained cratons for a similar interval.

5.6. Other potential paleomagnetic correlations: Neoproterozoic to Cambrian

While an older age for the Vindhyanchal Basin is our preferred interpretation, we understand that the Upper Vindhyan paleomagnetic pole is commonly treated as late Neoproterozoic to Cambrian in age. This is due in part to several apparent correlations between the Upper Vindhyan paleomagnetic pole and alleged similarly aged poles from various Gondwana elements. The Bhander and Rewa paleomagnetic pole has been placed on the Gondwana APW path by assuming a Neoproterozoic–Cambrian age and comparing them with the 547 ± 4 Ma Sinyai dolerite (Csd; Fig. 16) paleomagnetic pole (29°N, 139°E, $\alpha_{95} = 5.0°$) of Meert and Van der Voo (1996). This match has been used by many authors and seems reasonable given the equivocal age constraints on the Upper Vindhyan sequence. However, further investigation brings forward two lines of evidence that suggest that the comparison is not so simple. The robust 755 ± 3 Ma Mundine Well dyke (Amw; Fig. 16) paleomagnetic pole (45.3°N, 135.4°E, $\alpha_{95} = 5.0°$) from Australia actually correlates better to the 547 Ma Sinyai dolerite paleomagnetic pole than to the Upper Vindhyan, as illustrated by Fig. 16. The possibil-

Table 3
Paleomagnetic data used in this study

Study	Symbol	Age (Ma)	N	D	I	κ	α_{95}/A95	Pole Latitude*	Pole Longitude*
India									
Harohalli dykes (recalc Pradhan et al., in press)	Har	1192 ± 10	10 sites	2.3	83.6	34	8.4	24.9°N	78.0°E
Majhgawan kimberlite (Gregory et al., 2006)	Maj	1073 ± 13.7	22	37.5	−26.5	54	15.3	36.8°S	32.5°E
Bhander–Rewa (Athavale et al., 1972)	Bra	980–1070	18	49.0	−19.0	200	5.7	31.5°S	19.0°E
Bhander–Rewa (Klootwijk, 1973)	Brk	980–1070	37	207.5	37.0	137	5.5	48.5°S	33.5°E
Bhander–Rewa (McElhinny et al., 1978)	Brm	980–1070	21	203.0	8.1	17.5	11.1	51°S	37.8°E
Bhander–Rewa: This study	TS	980–1070	34 Sites	–	–	33	4.3	44°S	34.0°E
Malani Igneous province (Torsvik et al., 2001a,b)	Mal	771 ± 5	4 Studies	359.1	62.0	73.17	7.9	72.7°S	250.5°E
Australia									
Bangemell Basin sill (Wingate et al., 2002)	Abs	1071 ± 8	79	339.9	46.5	30	8.4	83.7°S	128.6°E
Alcurra dykes (Schmidt et al., 2006)	Aad	~1070	47	281.2	50.8	41.9	8.0	57.7°S	227.9°E
Mundine Well dykes (Wingate and Giddings, 2000)	Amw	775 ± 3	116	14.8	31.1	–	5.0	58°S	36.8°E
Yaltipena Fm (Sohl et al., 1999)	Ayf	600–610	36	204.0	−16.4	12.2	11.0	32°S	33.8°E
Elatina Fm (Sohl et al., 1999)	AYe	590–600	126	212.1	−16.9	9.9	6.2	24°S	30.4°E
Africa									
Sinyai dolerite (Meert and Van der Voo, 1996)	Csd	547 ± 4	42	241.0	20.0	20	5.0	64.3°S	31.7°E

*Euler Pole: Rotation to India coordinates	Lat	Long	Angle
Africa to India	29.6	36.1	56.8
Australia to India	11.07	183.48	−62.09

N: number of samples used unless indicated as sites or studies. *D*: mean declination; *I*: mean inclination, κ: kappa precision parameter, α_{95}/A95 = cone of 95% confidence about the mean direction or mean pole.

ity of a remagnetization of the Mundine Well dykes is unlikely, as a positive baked contact test suggests the primary nature of the magnetization (Wingate and Giddings, 2000). Placing the Upper Vindhyan near the Neoproterozoic–Cambrian boundary also reintroduces the lack of diagnostic global events recorded in the Upper Vindhyan, such as the glacial markers, definitive cap carbonates phosphorite deposits and definitive evidence for transitional faunas to the Cambrian expansion described in preceding sections.

Paleomagnetic data from the Elatina (Aef) and Yaltipena formations (Ayf) of Australia resemble the Upper Vindhyan paleomagnetic pole, as seen in Fig. 16. The Elatina formation is commonly associated with the Marinoan glaciation and is generally dated at ~635–645 Ma, and the Yaltipena formation lies stratigraphically beneath the Elatina (Schmidt and Williams, 1995; Sohl et al., 1999). The Elatina formation shows clear evidence of glaciation in the form of a basal diamictite, dropstones, and other diagnostic features of a coastal glaciomarine setting (Sohl et al., 1999). In contrast, the Bhander Group of India lacks such definite glaciogenic features (Prasad, 1984; Kumar et al., 2002). The primary tie between the Bhander Group and other "Snowball Earth" units is the negative $\delta^{13}C$ excursion used to label the Lakheri limestone as a cap carbonate. This correlation is questionable, however, as Ray et al. (2003) note that the excursion is not found in the Son Valley section of the Lakheri limestone. Furthermore, Banerjee et al. (2006) show that the observed $\delta^{13}C$ excursion in the Lhakheri limestone is facies related and our paleomagnetic data support previous correlations between the Rajasthan and Son Valley limestones (see also Kennedy, 1996). Lastly, Meert (2007) notes that the $\delta^{13}C$ curves for both the Sturtian and Marinoan glaciations require further geochronologic work to allow for usable correlations. New

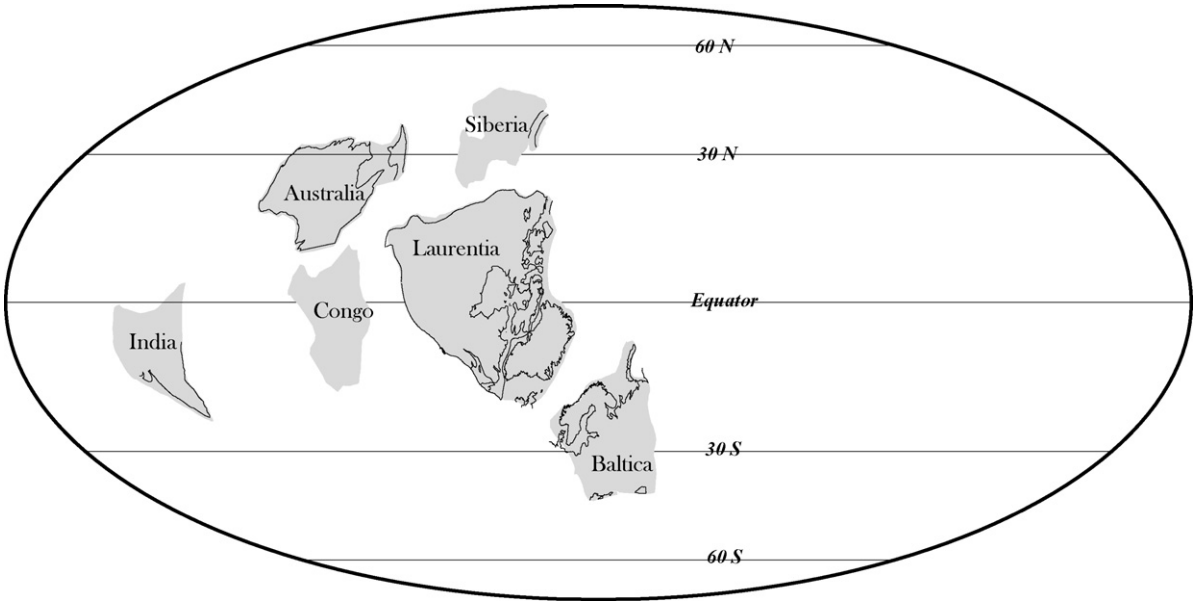

Fig. 17. Reconstruction at ca. 1150 Ma based on the Bhander–Rewa/Majghawan pole, the Bangamall Sills pole and Laurentian, Congo and Siberian poles given in Pesonen et al. (2003).

geochronology on the Edwardsburg (Windemere SuperGroup), Aralka (Australia), Tindelpina (Australia) and Merinjina (Australia) formations strongly suggest that the Sturtian glaciation was not a synchronous event (see Meert, 2007 for a summary).

The Upper Vindhyan paleomagnetic pole (44°N, 214.0° E; A95 = 4.3°) shows some similarity to the robust 755 Ma Mundine Well dyke paleomagnetic pole (45.3°N, 135.4°E, α_{95} = 5.0°) from Australia seen in Fig. 16 (Wingate and Giddings, 2000). Defining the age of the Upper Vindhyan sequence on the basis of this correlation is apparently supported by the $^{87}Sr/^{86}Sr$ data compiled by Kumar et al. (2002) and Ray et al. (2003), which assign a minimum age of 750–650 Ma to the Bhander–Lakheri limestone. Further investigation of paleomagnetic data for this interval yields an intriguing problem in relation to the age of Upper Vindhyan. The Malani Igneous province provides a key paleomagnetic pole (69.0°N, 83.2°E; dp = 8.8°, dm = 10.9°) at 771–750 Ma (Torsvik et al., 2001a,b; Gregory et al., submitted for publication). The directions and paleomagnetic pole provided by the Malani dataset differ sharply from the Upper Vindhyan paleomagnetic pole in terms of both position and paleolatitude (Fig. 16). The study regions for these poles both lie on the Aravalli-Bundelkhand craton, and are unlikely to have been separated by any great distance. Furthermore, the Malani paleomagnetic pole is separated from the Mundine Well dykes paleomagnetic pole. This separation between two robust paleomagnetic poles precludes any connection between the Aravalli-Bundelkhand craton and Australia in the ~750 Ma age range.

6. Conclusions

This study provides a refined paleomagnetic pole for the Upper Vindhyan sequence of the Vindhyanchal Basin at 44°N, 214.0°E (A95 = 4.3°). This paleomagnetic pole correlates well with the VGP generated from the Majhgawan kimberlite by Gregory et al. (2006) that lies at 36.8N, 212.5E (α_{95} = 15.3°). Age control on the Upper Vindhyan remains controversial. The 1073 ± 13.7 Ma Majhgawan kimberlite (Gregory et al., 2006) intrudes the Lower Vindhyan Semri Group and Kaimur sandstone and places limits on their age. The Bhander and Rewa Groups are unconstrained by reliable direct age dates. Detrital zircon geochronology helps to provide a maximum age control by identifying the youngest age population centered at 1020 Ma. Other age control is provided by $^{87}Sr/^{86}Sr$ isotope data correlated to global curves. The 650–750 Ma age assigned to the Lakheri–Bhander limestone by these correlations (Ray et al., 2003) fails to correspond well with the existing paleomagnetic data, such as the conflicting correlations between the well-dated robust Malani and Mundine Well dyke paleomagnetic poles. Fossil evidence provides yet another possible age control for the Upper Vindhyan paleomagnetic pole. We argue that the simplest interpretation for the age of the Bhander and Rewa Groups is that the pole is close to the age of Majhgawan kimberlite (i.e. between 1000 and 1070 Ma). Patranabis-Deb et al. (2007) make a similar 500 Ma revision to the age of the Chattisgarh Basin on the basis of direct dates (990, 1015, and 1020 Ma) on tuff layers near the top of that basin, suggesting that such a downward revision may be needed for other Purana Basins. The Purana Basins are recognized as having similar origins and ages, applying this older revision to the Vindhyanchal Basin by default. By assigning this age to the Bhander and Rewa Group, several interesting possibilities can be considered. The Upper Vindhyan paleomagnetic poles, along with the Majhgawan VGP, fail to correlate with Australian poles (e.g. Bangamall sills, Alcurra dykes) dated between 1070 and 1050 Ma. This suggests a separation between Australia and India at this time. If the Malani Igneous province and Mundine Well dykes paleomagnetic poles are considered, this separation is demonstrated to have lasted until ~750 Ma. These data support the idea that East Gondwana did not coalesce until the end Neoproterozoic–Cambrian transition, as suggested by Meert et al. (1995), Powell and Pisarevsky (2002), and Meert (2003).

Acknowledgements

This work was supported by a grant from the US National Science Foundation (EAR04-09101 to J.G.M.). We thank Abhijit Basu and Phil McCausland for thoughtful and careful reviews of this manuscript that help make it more readable and scientifically accurate.

Appendix A. Supplementary data

Supplementary data associated with this article can be found, in the online version, at doi:10.1016/j.precamres.2008.04.004.

References

Akhtar, K., 1996. Facies, sedimentation processes and environments in the Proterozoic Vindhyan Basin, India. In: Bhattacharyya, A. (Ed.), Recent Advances in Vindhyan Geology. Geological Society of India, Bangalore.
Auden, J.B., 1933. Vindhyan sedimentation in the Son Valley, Mirzapur district, memoir. Geol. Surv. India, 141–250.
Athavale, R.N., Hansraj, Asha, Verma, R.K., 1972. Palaeomagnetism and age of Bhander and Rewa sandstones from India. Geophys. J. R. Astronom. Soc. 28, 499–509.
Azmi, R.J., 1998. The discovery of Lower Cambrian small shelly fauna fossils and brachiopods from the Lower Vindhyan of Son Valley, central India. J. Geol. Soc. India 52, 381–389.
Banerjee, D.M., Mazumdar, A., 1999. On the Late Neoproterozoic-Early Cambrian transition events in parts of East Godwanaland. Gondwana Res 2, 199–211.
Banerjee, S., Bhattacharya, S.K., Sarkar, S., 2006. Carbon and oxygen isotopic compositions of the carbonate facies in the Vindhyan SuperGroup, central India. J. Earth Sys. Sci. 115, 113–134.
Bengtson, S., Belivanova, V., Rassmussen, B., Whitehouse, M.J., 2007. The Vindhyan enigma revisited. Geol. Soc. Am. Abstr. 39 (6), 331.
Biju-Sekhar, S., Pandit, M.K., Yokoyama, K., Santosh, M., 2000. Electron microprobe dating of the Ajitgarha and Barodiya granitoids, NW India; Implications on the evolution of the Delhi Fold Belt. J. Geosci. 45, 13–27.
Black, L.P., Kamo, S.L., Williams, I.S., Mundil, R., Davis, D.W., Korsch, R.J., Foudoulis, C., 2003. The application of SHRIMP to Phanerozoic geochronology; a critical appraisal of four zircon standards. Chem. Geol. 200, 171–188.
Bose, P.K., Sarkar, S., Chakrabarty, S., Banerjee, S., 2001. Overview of the Meso- to Neoproterozoic evolution of the Vindhyan Basin, central India. Sed. Geol. 141, 395–419.
Buick, I.S., Allen, C., Pandit, M., Rubatto, D., Hermann, J., 2006. The Proterozoic magmatic and metamorphic history of the Banded Gneiss Complex, central Rajasthan, India. LA-ICP-MS U–Pb zircon constraints. Precambrian Res. 151, 119–142.
Crawford, A.R., Compston, W., 1970. The age of the Vindhyan system of peninsular India. Q. J. Geol. Soc. Lond. 125, 351–371.
Chakrabarti, A., 1990. Traces and dubiotraces: examples from the so called Late Proterozoic silisiclastic rocks of the Vindhyan SuperGroup around Maihar, India. Precambrian Res. 47, 141–153.
Chakraborty, C., 2006. Proterozoic intracontinental basin: The Vindhyan example. J. Earth Syst. Sci. 115, 3–22.
Chakraborty, P.P., Banerjee, S., Das, N.G., Sarkar, S., Bose, P., 1996. Volcaniclastics and their sedimentological bearing in Proterozoic Kaimur and Rewa Groups in Central India. Mem. Geol. Soc. India 36, 59–76.
Chaudhuri, A.K., Mukhopadhyay, J., Patranabis-Deb, S., Chanda, S.K., 1999. The Neoproterozoic cratonic successions of peninsular India. Gondwana Res. 2, 213–225.
Chaudhuri, A.K., Saha, D., Deb, G.K., Deb, S.P., Mukherjee, M.K., Ghosh, G., 2002. The Purana basins of southern cratonic province of India- A case for Mesoproterozoic fossil rifts. Gondwana Res. 5, 23–33.
Collins, A.S., Pisarevsky, S.A., 2005. Amalgamating eastern Gondwana: The evolution of the circum-Indian orogens. Earth Sci. Rev. 71, 229–270.
Condon, D., Zhu, M.Y., Bowring, S., Wang, W., Wang, A.H., Jin, Y.G., 2005. U–Pb ages from the Neoproterozoic Doushantua Formation, China. Science 308, 95–98.
Dalziel, I.W.D., 1997. Neoproterozoic–Paleozoic geography and tectonics; review, hypothesis, environmental speculation. GSA Bull. 109, 16–42.
De, C., 2003. Possible organisms similar to Ediacaran forms of the Bhander Group, Vindhyan SuperGroup, Late Neoproterozoic of India. J. Asian Earth Sci. 21, 387–395.
De, C., 2006. Ediacara fossil assemblage in the Upper Vindhyans of Central India and its significance. J. Asian Earth Sci. 27, 660–683.
Deb, M., Thorpe, R.I., Krstic, D., Corfu, F., Davis, D.W., 2001. Zircon U–Pb and galena Pb isotope evidence for an approximate 1.0 Ga terrane constituting the western margin of the Aravalli-Delhi orogenic belt, northwestern India. Precambrian Res. 108, 195–213.

Deb, M., Thorpe, R., Krstic, D., 2002. Hindoli Group of rocks in the Eastern Fringe of the Aravalli–Delhi Orogenic belt—Archean secondary greenstone belt or Proterozoic supracrustals? Gondwana Res. 5, 879–883.
Dunlop, D.J., Argyle, K.S., 1991. Separating multidomain and single-domain like remanences in pseudo-single domain magnetites (215-540 nm) by low temperature demagnetization. J. Geophys. Res. 96, 2007–2017.
Fareeduddin, Kroner, A., 1998. Single zircon age constraints on the evolution of Rajasthan granulite. In: Paliwal, B.S. (Ed.), The Indian Precambrian. Scientific Publishers, Jodhpur, India, pp. 547–556.
Gray, D.R., Foster, D.A., Meert, J.G., Goscombe, B.D., Armstrong, R., Truow, R.A.J., Passchier, C.W. A Damaran perspective on the assembly of southwestern Gondwana. In: Pankhurst, R.J., Trouw, R.A.J, De Brito Neves, B.B., De Wit, M.J. (Eds.), West Gondwana: Pre- Cenozoic Correlations Across South Atlantic Region, Geological Society, London, Special Publication 294, p. 257–278.
Gregory, L.C., Meert, J.G., Pradhan, V., Pandit, M.K., Tamrat, E., Malone, S.J., 2006. A paleomagnetic and geochronologic study of the Majhgawan Kimberlite, India: Implications for the age of the Vindhyan SuperGroup. Precambrian Res. 149, 65–75.
Gregory, L.C., Meert, J.G., Bingen, B.A., Pandit, M.K., Torsvik, T.H. Paleomagentism and geochronology of the Malani igneous suite, Northwest India: implications for the configuration of Rodinia and the assembly of Gondwana. Precambrian Res., submitted for publication.
Halls, H.C., Kumar, A., Srinivasan, R., Hamilton, M.A., 2007. Paleomagnetism and U–Pb geochronology of easterly trending dykes in the Dharwar craton, India: Feldspar clouding, radiating dyke swarms and the position of India at 2.37 Ga. Precambrian Res. 155, 47–68.
Heron, A.M., 1932. The Vindhyans of western Rajputana. Rec. Geol. Sur. India. 65, 457–489.
Heron, A.M., 1936. Geology of southeastern Mewar, Rajputana. Rec. Geol. Sur. India. 63, 1–130.
Jiang, G., Sohl, L.E., Christie-Blick, N., 2003. Neoproterozoic stratigraphic comparison of the Lesser Himalaya (India) and Yangtze Block (south China): Paleogeographic implications. Geology 31, 917–920.
Kendall, B., Creaser, R.A., Selby, D., 2006. Re-Os geochronology of postglacial black shales in Australia: Constraints on the timing of the "Sturtian" glaciation. Geology 34, 729–732.
Kennedy, M.J., 1996. Stratigraphy, sedimentology, and isotope geochemistry of Australian Neoproterozoic postglacial cap dolostones: Deglaciation, delta C-13 excursions, and carbonate precipitation. J. Sed. Res. 66, 1050–1064.
Klootwijk, C.T., 1973. Palaeomagnetism of upper Bhander sandstones from central India and implications for a tentative Cambrian Gondwanaland reconstruction. Tectonophysics 18, 123–145.
Klootwijk, C.T., Nazirullah, R., de Jong, K.A., 1986. Paleomagnetic constraints on formation of the Mianwali re-entrant, Trans-Indus and Western Salt Range, Pakistan. Earth Planet. Sci. Lett. 80, 394–414.
Kumar, S., 2001. Mesoproterozoic megafossil Chuaria-Tawuia association may represent parts of a multicellular plant, Vindhyan Supergroup, central India. Precam. Res. 106, 187–211.
Kumar, A., Padmakumari, V.M., Murthy, D.S.M., Gopalan, K., 1993. Rb–Sr Ages of Proterozic kimberlites of India: Evidence for contemperaneous emplacement. Precambrian Res. 62, 227–232.
Kumar, B., Das Sharma, S., Sreenivas, B., Dayal, A.M., Rao, M.N., Dubey, N., Chawla, B.R., 2002. Carbon, oxygen and strontium isotope geochemistry of Proterozoic carbonate rocks of the Vindhyan Basin, central India. Precambrian Res. 113, 43–63.
Kumar, S., Srivastava, P., 1997. A note on the carbonaceous megafossils from the Neoproterozoic Bhander Group, Maihar area, Madhya Pradesh. J. Paleontol. Soc. India 42, 141–146.
Kumar, S., Srivastava, P., 2003. Carbonaceous marcrofossils from the Neoproterozoic Bhander Group, central India. J. Paleontol. Soc. India 48, 139–154.
Ludwig, K.R., 2000. Isoplot/Ex Version 2.4. A Geochronological Toolkit for Microsoft Excel. 1.a. Berkley Geochronological Centre Special Publication, Berkley.
Mathur, S.M., 1981. A revision of the stratigraphy of the Vindhyan Supergroup in the Son Valley, Mirzapur district, Uttar Pradesh, Geol. Survey of India Misc Publ. #50, 7–20.
Mazumdar, R., Bose, P.K., Sarkar, S., 2000. A commentary on the tectanosedimentary record of pre-2.0 Ga continental growth in India vis-à-vis possible pre-Gondwana Afro Indian supercontinent. J. Afr. Earth Sci. 30, 201–217.
Mazumdar, R., Banerjee, D.M., 2001. Regional variations in the carbon isotopic composition of phosphorite from the Early Cambrian Lower Tal formation, Mussoorie Hills, India. Chem. Geol. 175, 5–15.
McElhinny, M.W., Cowley, J.A., Edwards, D.J., 1978. Palaeomagnetism of some rocks from peninsular India and Kashmir. Tectonophysics 50, 41–54.
McFadden, P.L., McElhinny, M.W., 1990. Classification of the reversal test in paleomagnetism. Geophys. J. Int. 103, 725–729.
Meert, J.G., 2001. Growing Gondwana and rethinking Rodinia: a paleomagnetic perspective. Gondwana Res. 4, 279–288.
Meert, J.G., 2003. A Synopsis of events related to the assembly of East Gondwana. Precambrian Res. 362, 1–40.
Meert, J.G., 2007. Testing the Neoproterozoic glacial models. Gondwana Res. 11, 573–574.
Meert, J.G., Lieberman, B.S., 2008. The Neoproterozoic assembly of Gondwana and its relationship to the Ediacaran-Cambrian radiation. Gondwana Res., doi:10.1016/j.gr.2007.06.007.
Meert, J.G., Torsvik, T.H., 2003. The making and unmaking of a supercontinent: Rodinia revisted. Tectonophysics 375, 261–288.
Meert, J.G., Powell, C.M.A., 2001. Assembly and Breakup of Rodinia. Precambrian Res. 110, 1–8.
Meert, J.G., Van der Voo, R., 1996. Paleomagnetic and $^{40}Ar/^{39}Ar$ study of the Sinyai dolerite, Kenya: implications for Gondwana assembly. J. Geol. 104, 131–142.
Meert, J.G., Van der Voo, R., Ayub, S., 1995. Paleomagnetic investigation of the Neoproterozoic Gagwe lavas and Mbozi complex, Tanzania and the assembly of Gondwana. Precambrian Res. 74, 225–244.
Meert, J.G., Pandit, M.K., Pradhan, V., Gregory, L.C., Malone, S., Torsvik, T.H., Bingen, B., 2008. India's changing place in global Neoproterozoic reconstructions: New geochronologic constraints on key paleomagnetic poles. In: Int. Ass. Gondwana Res. Conference Series, vol. 5, pp. 23–24.
Miller, K.C., Hargraves, R.B., 1994. Paleomagnetism of some Indian kimberlites and lamporites. Precambrian Res. 69, 259–267.
Mitra, N.D., 1996. Some problems of Vindhyan geology. Mem. Geol. Soc. India 36, 137–155.
Mondal, M.E.A., Goswami, J.N., Deomurari, M.P., Sharma, K.K., 2002. Ion microprobe 207Pb/206Pb ages of zircons from the Bundelkhand Massif, northern India: implications for crustal evolution of the Bundelkhand-Aravalli supercontinent. Precambrian Res. 117, 85–100.
Norton, I.O., Sclater, J.G., 1979. A model for the evolution of the Indian Ocean and the breakup of Gondwana. J. Geophys. Res. 84, 6803–6830.
Oldham, R D., 1893. Manual of Geology, second ed. Calcutta, India.
Paul, D.K., Potts, P.J., Gibson, I.L., Harris, P.G., 1975. Rare-earth abundances in Indian kimberlites. Earth Planet. Sci. Lett. 25, 151–158.
Paul, D.K., 1979. Isotopic composition of strontium in Indian kimberlites. Geochim. Cosmochim. Acta 43, 389–394.
Paces, J.B., Miller, J.D., 1993. Precise U–Pb ages for the Duluth Complex and related mafic intrusions, Northeastern Minnesota: Geochronological insights to physical, petrogenetic, paleomagnetic and tectonomagmatic processes associated with the 1.1 Ga Midcontinent Rift system. Journal of Geophysical Research 98, 13997–14013.
Pascoe, H.S., 1959. A Manual on the Geology of India and Burma, vol. 2., third ed. Geologic Survey of India, pp. 1–485.
Patranabis-Deb, S., Bickford, M.E., Hill, B., Chaudhuri, A.K., Basu, A., 2007. SHRIMP ages of zircon in the uppermost tuff in Chattisgarh Basin in central India require up to 500 Ma adjustment in Indian Proterozoic stratigraphy. J. Geol. 115, 407–416.
Pesonen, L.J., Elming, S.A., Mertanen, S., Pisarevsky, S., D'Agrella, M.S., Meert, J.G., Schmidt, P.W., Abrahamsen, N., Bylund, G., 2003. Paleomagnetic configuration of continents during the Proterozoic. Tectonophysics 375, 289–324.
Poornachandra Rao, G.V.S., Mallikharjuna Rao, J., Rajendra Presed, N.P., Venkatewarlu, M., Srinivasa Rao, B., Ravi Prakash, S., 2005. Tectonics and correlation of Upper Kaimur Group sandstones by their paleomagnetic study. J. Ind. Geophys. Union 9, 83–95.
Powell, C.McA., Pisarevsky, S.A., 2002. Late Neoproterozoic assembly of east Gondwana. Geology 3, 3–6.
Pradhan, V.R., Pandit, M.K., Meert, J.G. A cautionary note on the age of the paleomagnetic pole obtained from the Harohalli dyke swarms, Dharwar craton, India. In: Srivasatava, et al. (Eds.), Indian Dykes. Narosa Publishing House, New Delhi, India, in press.
Prasad, B., 1984. Geology, sedimentation and paleogeography of the Vindhyan SuperGroup, southeastern Rajasthan. Mem. Geol. Soc. India 116, 1–58, part 2.
Prasad, B.R., Rao, V.V., 2006. Deep seismic reflection study over the Vindhyans of Rajasthan: implications for the geophysical setting of the basin. J. Earth Syst. Sci. 115, 135–147.
Radhakrishna, T., Mathew, J., 1996. Late Precambrian (850–800 Ma) paleomagnetic pole for the south Indian shield from the Harohalli alkaline dykes: geotectonic implications for Gondwana reconstructions. Precambrian Res. 80, 77–87.
Rai, V., Shukla, M., Gautam Vibhuti, R., 1997. Discovery of carbonaceous megafossils (Chuaria-Tawuia assemblage) from the Neoproterozoic Vindhyan succession (Rewa Group), Allahabad, India. Curr. Sci. 73, 783–788.
Ram, J., Shukla, S.N., Pramanik, A.G., Varma, B.K., Chandra, G., Murthy, M.S.N., 1996. Recent investigations in the Vindhyan basin: implications for basin tectonics. Mem. Geol. Soc. India 36, 267–286.
Rasmussen, B., Bose, P.K., Sakar, S., Banerjee, S., Fletcher, I.R., McNaughton, N.J., 2002a. 1.6 Ga U–Pb zircon age for the Chorhat Sandstone, Lower Vindhyan, India: possible implications for the early evolution of animals. Geology 20, 103–106.
Rasmussen, B., Fletcher, I.R., Bengtson, S., McNaughton, N.J., 2002b. Discoidal impressions and trace-like fossils more than 1200 million years old. Science 296, 1112–1115.
Rasmussen, B., Fletcher, I.R., Bengtson, S., McNaughton, N.J., 2004. SHRIMP U–Pb dating of diagenetic xenotime in the Sterling Range Formation, Western Australia: 1.8 billion year minimum age for the Sterling Biota. Precambrian Res. 133, 329–337.
Rau Soni, T.K., 2003. Diamondiferous Vindhyan conglomerates and their provenance: a critical study. Indian Min. 37, 22–30.
Ray, J., 2006. Age of the Vindhyan SuperGroup: a review of recent findings. J. Earth Syst. Sci. 115, 149–160.
Ray, J.S., Martin, M.W., Veizer, J., Bowring, S.A., 2002. U–Pb Zircon dating and Sr isotope systematic of the Vindhyan SuperGroup, India. Geology 30, 131–134.
Ray, J.S., Veizer, J., Davis, W.J., 2003. C, O, Sr and Pb isotope systematics of carbonate sequences of the Vindhyan SuperGroup, India: Age, diagenesis, correlations, and implications for global events. Precambrian Res. 121, 103–140.

Raghav, K.S., De, C., Jain, R.L., 2005. The first record of Vendian Medusoids and trace fossil-bearing algal matgrounds from the basal part of the Marwar SuperGroup of Rajasthan, India. Indian Miner. 59, 22–30.
Rogers, J.J.W., Unrug, R., Sultan, M., 1995. Tectonic assembly of Gondwana. J. Geodynam. 19, 1–34.
Roy, A.B., 2001. Neoproterozoic crustal Evolution of Northwestern Indian Shield: Implications on break up and assembly of supercontinents. Gondwana Res. 4, 289–306.
Sahasrabudhe, P.W., Mishra, D.C., 1966. Paleomagnetism of Vindhyan Rocks of India. Bull. Natl. Geophys. Res. Inst. Hyderabad 4, 49–55.
Sarangi, S., Gopalan, K., Kumar, S., 2004. Pb–Pb age of earliest megascopic, eukaryotic alga bearing Rhotas formation, Vindhyan SuperGroup, India: implications for Precambrian atmospheric oxygen evolution. Precambrian Res. 121, 107–121.
Sarkar, A., Paul, D.K., Potts, P.J., 1995. Geochronology and geochemistry of the mid-Archean trondjemitic gneisses from the Bundelkhand craton, central India. In: Saha, A.K. (Ed.), Recent Researches in Geology and Geophysics of the Precambrian. Recent Researches in Geology, vol. 16, pp. 76–92.
Schmidt, P.W., Williams, G.E., 1995. The Neoproterozoic climatic paradox – Equatorial paleolatitude for Marinoan glaciation near sea-level in South Australia. Earth Planet. Sci. Lett. 134, 107–124.
Schmidt, P.W., Williams, G.E., Camacho, A., Lee, J.K.W., 2006. Assembly of Proterozoic Australia: implications of a revised pole for the ~1070 Ma Alcurra Dyke swarm, central Australia. Geophys. J. Int. 167, 626–634.
Seilacher, A., Bose, P.K., Pfluger, F., 1998. Triploblastic animals more than 1 billion years ago: trace fossil evidence from India. Science 282, 80–83.
Shen, Y., Schidlowski, M., Chu, X., 2000. Biogeochemical approach to understanding phosphogenic events in the terminal Proterozoic to Cambrian. Palaeogeography, palaeoclimatology. Palaeoecology 158, 99–108.
Smith, C.B., 1992. The age of the Majhgawan pipe, India. Scott Smith Petrol., 9.
Sohl, L.E., Christie-Blick, N., Kent, D.V., 1999. Paleomagnetic polarity reversals in Marinoan (ca. 600 Ma) glacial deposits of Australia; implications for the duration of low-latitude glaciation in the Neoproterozoic time. GSA Bull. 111, 1120–1139.
Squire, R.J., Campbell, I.H., Allen, C.M., Wilson, C.J.L., 2006. Did the Transgondwanan supermountain trigger the explosive radiation of animals on Earth? Earth Planet. Sci. Lett. 250, 116–135.
Srivastava, A.P., Rajagopalan, G., 1988. F-T Ages of the Vindhyan Glauconitic sandstone beds exposed around the Rawatbhata area, Rajasthan. J. Geol. Soc. India 32, 527–529.
Torsvik, T.H., Briden, J.C., Smethurst, M.A., 2000. IAPD 2000. Norwegian Geophysical Union.
Torsvik, T.H., Carter, L., Ashwal, L.D., Bhushan, S.K., Pandit, M.K., Jamtveit, B., 2001a. Rodinia refined or obscured: Paleomagnetism of the Malani Igneous Suite (NW India). Precambrian Res. 108, 319–333.
Torsvik, T.H., Ashwal, L.D., Tucker, R.D., Eide, E.A., 2001b. Neoproterozoic geochronology and paleogeography of the Seychelles microcontinent: the India link. Precambrian Res. 110, 47–59.
Tugarinov, A.I., Shanin, L.L., Kazakow, G.A., Arakelyantis, M.M., 1965. On the Glauconite ages of the Vindhyan system (India). Geokhmiya 6, 652–660.
Veevers, J.J., 2004. Gondwanaland from 650–500 Ma assembly through 320 Ma merger in Pangea to 185–100 Ma breakup: supercontinental tectonics via stratigraphy and radiometric dating. Earth Sci. Rev. 68, 1–132.
Verma, P.K., 1996. Evolution and age of the Great Boundary Fault of Rajasthan. Mem. Geol. Soc. India 36, 137–155.
Venkatachala, B.S., Mukund, S., Shukla, M., 1996. Age and Life of the Vindhyans- Facts and Conjectures. Mem. Geol. Soc. India 36, 137–155.
Vinogradov, A.P., Tugarinov, A.I., Zhikov, C.I., Stanikova, N.I., Bibikova, E.V., Khorre, K., 1964. Geochronology of the Indian Precambrian. Report of the 22nd International Congress, New Dehli, vol. 10, pp. 553–567.
Waggoner, B., 1999. Biogeographic analyses of the Ediacara biota: A conflict with paleotectonic reconstructions. Paleobiology 25, 440–458.
Waggoner, B., 2003. The Ediacaran biotas in space and time. Integr. Compar. Biol. 43, 104–113.
Weil, A.B., Van der Voo, R., Mac Niocall, C., Meert, J.G., 1998. The Proterozoic supercontinent Rodinia: paleomagnetically derived reconstructions for 1100 to 800 Ma. Earth Planet. Sci. Lett. 154, 13–24.
Williams, I.S., 1998. U–Th–Pb geochronology by electron microprobe. In: McKibben, M.A., et al. (Eds.), Applications of Micro Analytical Techniques to Understanding Mineralizing Processes: Reviews in Economic Geology, vol. 7, pp. 1–35.
Wingate, M.T.D., Giddings, J.W., 2000. Age and paleomagnetism of the Mundine Well dyke swarm, Western Australia; implications for an Australia-Laurentia connection at 755 Ma. Precambrian Res. 100, 335–357.
Wingate, M.T.D., Pisarevsky, S.A., Evans, D.A.D., 2002. Rodinia connection between Australia and Laurentia; no SWEAT, no AUSWUS? Terra Nova 14, 121–128.
Xiao, L., Zhang, H., Ni, P., Xiang, H., Liu, X., 2007. LA-ICP-MS U–Pb zircon geochronology of early Neoproterozoic mafic-intermediate intrusions from NW margin of the Yangtze Block, South China: Implication for tectonic evolution. Precambrian Res. 154, 221–235.